

BRIEF DEFINITIVE REPORT

Respiratory viral infections in otherwise healthy humans with inherited IRF7 deficiency

Tessa Mollie Campbell^{1*}, Zhiyong Liu^{2*}, Qian Zhang^{2,3,4*}, Marcela Moncada-Velez², Laura E. Covill¹, Peng Zhang², Ilad Alavi Darazam^{5,6}, Paul Bastard^{2,3,4,27}, Lucy Bizien^{3,4}, Giorgia Bucciol^{7,8}, Sara Lind Enoksson^{9,10}, Emmanuelle Jouanguy^{2,3,4}, Şemsi Nur Karabela¹¹, Taushif Khan¹², Yasemin Kendir-Demirkol², Andres Augusto Arias^{2,13,14}, Davood Mansouri^{15,16}, Per Marits^{9,10}, Nico Marr¹², Isabelle Migeotte¹⁷, Leen Moens⁷, Tayfun Ozcelik¹⁸, Isabelle Pellier¹⁹, Anton Sendel⁹, Sevtap Şenoğlu¹¹, Mohammad Shahrooei^{20,21}, C.I. Edvard Smith^{22,23}, Isabelle Vandernoot¹⁷, Karen Willekens²⁴, Kadriye Kart Yaşar¹¹, COVID Human Genetic Effort, Peter Bergman^{22,25}, Laurent Abel^{2,3,4}, Aurélie Cobat^{2,3,4}, Jean-Laurent Casanova^{2,3,4,26,27**}, Isabelle Meyts^{7,8**}, and Yenan T. Bryceson^{1,9,28**}

Autosomal recessive IRF7 deficiency was previously reported in three patients with single critical influenza or COVID-19 pneumonia episodes. The patients' fibroblasts and plasmacytoid dendritic cells produced no detectable type I and III IFNs, except IFN-β. Having discovered four new patients, we describe the genetic, immunological, and clinical features of seven IRF7-deficient patients from six families and five ancestries. Five were homozygous and two were compound heterozygous for IRF7 variants. Patients typically had one episode of pulmonary viral disease. Age at onset was surprisingly broad, from 6 mo to 50 yr (mean age 29 yr). The respiratory viruses implicated included SARS-CoV-2, influenza virus, respiratory syncytial virus, and adenovirus. Serological analyses indicated previous infections with many common viruses. Cellular analyses revealed strong antiviral immunity and expanded populations of influenza- and SARS-CoV-2-specific memory CD4⁺ and CD8⁺ T cells. IRF7-deficient individuals are prone to viral infections of the respiratory tract but are otherwise healthy, potentially due to residual IFN-β and compensatory adaptive immunity.

¹Center for Hematology and Regenerative Medicine, Department of Medicine, Karolinska Institutet, Stockholm, Sweden; ²St. Giles Laboratory of Human Genetics of Infectious Diseases, Rockefeller Branch, Rockefeller University, New York, NY; ³Laboratory of Human Genetics of Infectious Diseases, Necker Branch, INSERM U1163, Necker Hospital for Sick Children, Paris, France; ⁴University Paris Cité, Imagine Institute, Paris, France; ⁵Department of Infectious Diseases and Tropical Medicine, Lohman Hakim Hospital, Shahid Beheshti University of Medical Sciences, Tehran, Iran; ⁶Infectious Diseases and Tropical Medicine Research Center, Shahid Beheshti University of Medical Sciences, Tehran, Iran; ⁷Department of Microbiology, Immunology and Transplantation, Laboratory of Inborn Errors of Immunity, KU Leuven, Leuven, Belgium; ⁸Department of Pediatrics, University Hospitals Leuven, Leuven, Belgium; ⁹Department of Clinical Immunology and Transfusion Medicine, Karolinska University Hospital, Stockholm, Sweden; ¹⁰Department of Clinical Science, Intervention and Technology, Karolinska Institutet, Stockholm, Sweden; ¹¹Department of Infectious Diseases and Clinical Microbiology, Bakirkoy Dr. Sadi Konuk Training and Research Hospital, University of Health Sciences, Istanbul, Turkey; ¹²Department of Human Immunology, Research Branch, Sidra Medicine, Doha, Qatar; ¹³Primary Immunodeficiencies Group, University of Antioquia UdeA, Medellín, Colombia; ¹⁴School of Microbiology, University of Antioquia UdeA, Medellín, Colombia; ¹⁵Department of Clinical Immunology and Infectious Diseases, National Research Institute of Tuberculosis and Lung Diseases, Shahid Beheshti University of Medical Sciences, Tehran, Iran; ¹⁶The Clinical Tuberculosis and Epidemiology Research Center, National Research Institute of Tuberculosis and Lung Diseases, Masih Daneshvari Hospital, Shahid Beheshti University of Medical Sciences, Tehran, Iran; ¹⁷Centre de Génétique Humaine de l'Université Libre de Bruxelles, Hôpital Erasme, Brussels, Belgium; ¹⁸Department of Molecular Biology and Genetics, Bilkent University, Bilkent-Ankara, Turkey; ¹⁹Université d'Angers, INSERM, CNRS, CRCl²NA, Pediatric Immuno-Hemato-oncology Unit, CHU Angers, Angers, France; ²⁰Specialized Immunology Laboratory of Dr. Shahrooei, Sina Medical Complex, Ahvaz, Iran; ²¹Department of Microbiology and Immunology, Clinical and Diagnostic Immunology, KU Leuven, Leuven, Belgium; ²²Department of Infectious Diseases, The Immunodeficiency Unit, Karolinska University Hospital, Stockholm, Sweden; ²³Department of Laboratory Medicine, Translational Research Center Karolinska, Karolinska Institutet, Stockholm, Sweden; ²⁴Department of Molecular Genetics, University Hospitals Leuven, Leuven, Belgium; ²⁵Department of Laboratory Medicine, Division of Clinical Microbiology, Karolinska Institutet, Stockholm, Sweden; ²⁶Howard Hughes Medical Institute, New York, NY; ²⁷Department of Pediatrics, Necker Hospital for Sick Children, Paris, France; ²⁸Broegelmann Laboratory, Department of Clinical Sciences, University of Bergen, Bergen, Norway.

*T.M. Campbell, Z. Liu, and Q. Zhang contributed equally to this paper; **J.-L. Casanova, I. Meyts, and Y.T. Bryceson contributed equally to this paper. Correspondence to Yenan T. Bryceson: yanan.bryceson@ki.se; Jean-Laurent Casanova: casanova@mail.rockefeller.edu; Qian Zhang: qzhang02@rockefeller.edu

COVID Human Genetic Effort authors: L. Abel, A. Aiuti, S. Al-Muhsen, F. Al-Mulla, M.S. Anderson, E. Andreaskos, A.A. Arias, H. Baris Feldman, A. Belot, C.M. Biggs, D. Bogunovic, A. Bolze, A. Bondarenko, A.A. Bousfiha, P. Brodin, Y. Bryceson, C.D. Bustamante, M.J. Butte, G. Casari, J. Christodoulou, A. Condino-Neto, S.N. Constantinescu, M.A. Cooper, C.L. Dalgard, M. Desai, B.A. Drolet, J. El Baghdadi, S. Espinosa-Padilla, J. Fellay, C. Flores, J.L. Franco, A. Froidure, P.K. Gregersen, B. Grimbacher, F. Haerynck, D. Hagin, R. Halwani, L. Hammarström, J.R. Heath, S.E. Henrickson, E.W.Y. Hsieh, E. Husebye, K. Imai, Y. Itan, E.D. Jarvis, T. Karamitros, K. Kisand, C.-L. Ku, Y.-L. Lau, Y. Ling, C.L. Lucas, T. Maniatis, D. Mansouri, L. Maródi, I. Meyts, J.D. Milner, K. Mironska, T.H. Mogensen, T. Morio, L.F.P. Ng, L.D. Notarangelo, A. Novelli, G. Novelli, C. O'Farrelly, S. Okada, K. Okamoto, T. Ozcelik, Q. Pan-Hammarström, M. Papadaki, J.W. Pape, R. Perez de Diego, D.S. Perlin, G. Pesole, A.M. Planas, C. Prando, A. Pujol, L. Quintana-Murci, S. Ramaswamy, L. Renia, I. Resnick, C. Rodríguez-Gallego, V. Sancho-Shimizu, A. Sediva, M.R.J. Seppänen, M. Shahrooei, A. Shcherbina, O. Slaby, A.L. Snow, P. Soler-Palacin, A.N. Spaan, I. Tancevski, S.G. Tangye, A. Abou Tayoun, S.E. Turvey, K.M.F. Uddin, M.J. Uddin, D. van de Beek, D.C. Vinh, H. von Bernuth, J. Wauters, M. Zatz, P. Zawadzki, H.C. Su, and J.-L. Casanova. Affiliations are listed at the end of the PDF.

© 2022 Campbell et al. This article is available under a Creative Commons License (Attribution 4.0 International, as described at <https://creativecommons.org/licenses/by/4.0/>).

Introduction

Human type I IFN-mediated immunity provides an intrinsic, innate first line of defense against invading viruses (Lazear et al., 2019; Schneider et al., 2014). The 17 type I IFN genes encode 13 forms of IFN- α , IFN- β , IFN- ϵ , IFN- κ , and IFN- ω . All nucleated cells can produce IFN- β upon sensing viral infection, and this contributes to the induction of other type I IFNs. During viral infections, plasmacytoid dendritic cells (pDCs) produce large quantities of IFN- α and - ω (Cella et al., 1999; Reizis, 2019; Siegal et al., 1999). IFN- κ and IFN- ϵ are preferentially expressed in the skin and reproductive tract, respectively, and are three orders of magnitude less potent than IFN- α 2 (Fung et al., 2013; Harris et al., 2018; LaFleur et al., 2001). Nucleated cells express type I IFN receptors, whereupon stimulation induces the transcription of type I IFN genes and other IFN-stimulated genes (ISGs), most of which promote antiviral immunity (Schoggins, 2019). Notably, however, human pluripotent stem cells constitutively express ISGs and display attenuated induction of ISGs upon type I IFN stimulation (Hong and Carmichael, 2013; Wu et al., 2018).

Ifnar1 or *Ifnar2* knockout mice that lack the type I IFN receptor are susceptible to many experimental infections, but an unexpected pattern is emerging in humans, with the corresponding deficits seeming to confer vulnerability to a narrower range of viruses (Duncan et al., 2021; Meyts and Casanova, 2021). Autosomal recessive (AR) IFNAR1 and IFNAR2 deficiencies have been reported in 16 and 9 patients, respectively (Abolhassani et al., 2022; Bastard et al., 2022; Bastard et al., 2021; Duncan et al., 2015; Duncan et al., 2022; Gothe et al., 2020; Hernandez et al., 2019; Zhang et al., 2020). Patients with inherited STAT2 or IRF9 deficiency lack ISG factor 3 (ISGF-3)—a transcription factor complex consisting of STAT1, STAT2, and IRF9 that normally induces ISG expression in response to type I and type III IFNs—but these patients have a similarly narrower range of viral susceptibility (Alosaimi et al., 2019; Hambleton et al., 2013; Hernandez et al., 2018; Moens et al., 2017).

Patients with an apparent complete absence of type I IFN immunity (IFNAR1, IFNAR2) or of ISGF-3 (STAT2, IRF9) are prone to adverse reactions to live attenuated viral vaccines, such as yellow fever virus 17D (YFV-17D) and the measles, mumps, and rubella virus (MMR) vaccine, and are also susceptible to HSV-1, encephalitis, and critical influenza or COVID-19 pneumonia (Abolhassani et al., 2022; Alosaimi et al., 2019; Bastard et al., 2021; Bastard et al., 2022; Duncan et al., 2015; Duncan et al., 2022; Hambleton et al., 2013; Hernandez et al., 2019; Hernandez et al., 2018; Moens et al., 2017; Zhang et al., 2020). The clinical penetrance of such infections in patients with type I IFN deficiencies remains unclear. These patients seem to be otherwise normally resistant to a number of common viruses. By contrast, AR complete and partial STAT1-deficient patients, with impairments of both ISGF-3 and γ -activated factor and, thus, unresponsive to type I, II, and III IFNs, are prone to various viral and intramacrophagic infections, resulting in early-onset disease following a devastating course (Boehmer et al., 2020; Burns et al., 2016; Chapgier et al., 2006; Dupuis et al., 2003; Le Voyer et al., 2021; Sakata et al., 2020; Vairo et al., 2011).

IRFs are a family of transcription factors initially identified on the basis of their ability to promote type I IFN production

(Miyamoto et al., 1988). IRF3 and IRF7 have been implicated in the transcription of type I IFN genes downstream from viral sensors, whereas other members of the IRF family promote the transcription of a subset of ISGs (e.g., IRF9) or regulate leukocyte development and differentiation (e.g., IRF8). These IRFs typically bind regulatory DNA elements similar to those bound by ISGF-3 (IFN-stimulated response element boxes). Studies of knockout mice have revealed a key role for IRF7 in the production of type I and III IFNs (Honda et al., 2005). These studies also showed that pDCs are the most potent type I and III IFN-producing cells, because of their markedly high levels of constitutive IRF7 expression (Colonna et al., 2004; Honda and Taniguchi, 2006; Liu, 2001; Reizis, 2019). *Irif7*-knockout mice are much more susceptible to fatal HSV-1, encephalomyocarditis virus, and influenza A virus (IAV) infections than either WT or *Irif7*-knockout mice, indicating a requirement for IRF7 in immunity to both DNA and RNA viruses (Hatesuer et al., 2017; Honda et al., 2005).

In humans, a 2.5-yr-old child with life-threatening influenza virus pneumonia was found to be compound heterozygous for loss-of-function (LoF) *IRF7* variants (Ciancanelli et al., 2015). This case confirmed the requirement for IRF7 for the induction of all type I and III IFNs, with the exception of IFN- β . More recently, two unrelated and previously healthy adults presented with life-threatening COVID-19 pneumonia due to inherited IRF7 deficiency (Zhang et al., 2020). Surprisingly, neither of these patients presented any clinically severe viral infections until the ages of 49 and 50 yr. This raises important questions regarding the requirement for IRF7-dependent type I and III IFNs for human immunity to viruses. With brief descriptions of only three patients, the range of severe viral infections and the individual penetrance of each viral infection in patients with inherited IRF7 deficiency remained unclear. Here, we studied the genetic, immunological, and clinical features of an international cohort of seven patients from six kindreds and five ancestries with AR IRF7 deficiency, including the three previously described patients.

Results and discussion

Patients with biallelic rare *IRF7* variants

In 2015, we reported AR IRF7 deficiency in a single patient with life-threatening influenza pneumonia (P1, F410V;Q421X; Ciancanelli et al., 2015). In 2020, we reported another two patients with AR IRF7 deficiency (P2, P364AfsX38;P364AfsX38 and P3, D117N;M371V) and life-threatening COVID-19 pneumonia, providing proof-of-principle that critical influenza and COVID-19 pneumonia can be allelic (Casanova and Abel, 2021; Zhang et al., 2022; Zhang et al., 2020). We have now performed whole-exome sequencing (WES) or whole-genome sequencing on the COVID Human Genetic Effort cohort of 927 adult patients with critical COVID-19 pneumonia (Casanova et al., 2020). We have also analyzed a cohort of 107 patients with severe influenza pneumonia. We searched for patients with biallelic very rare variants of *IRF7* (minor allele frequency [MAF] <0.001).

In addition to the three previously reported patients with critical influenza or COVID-19 pneumonia, we identified one

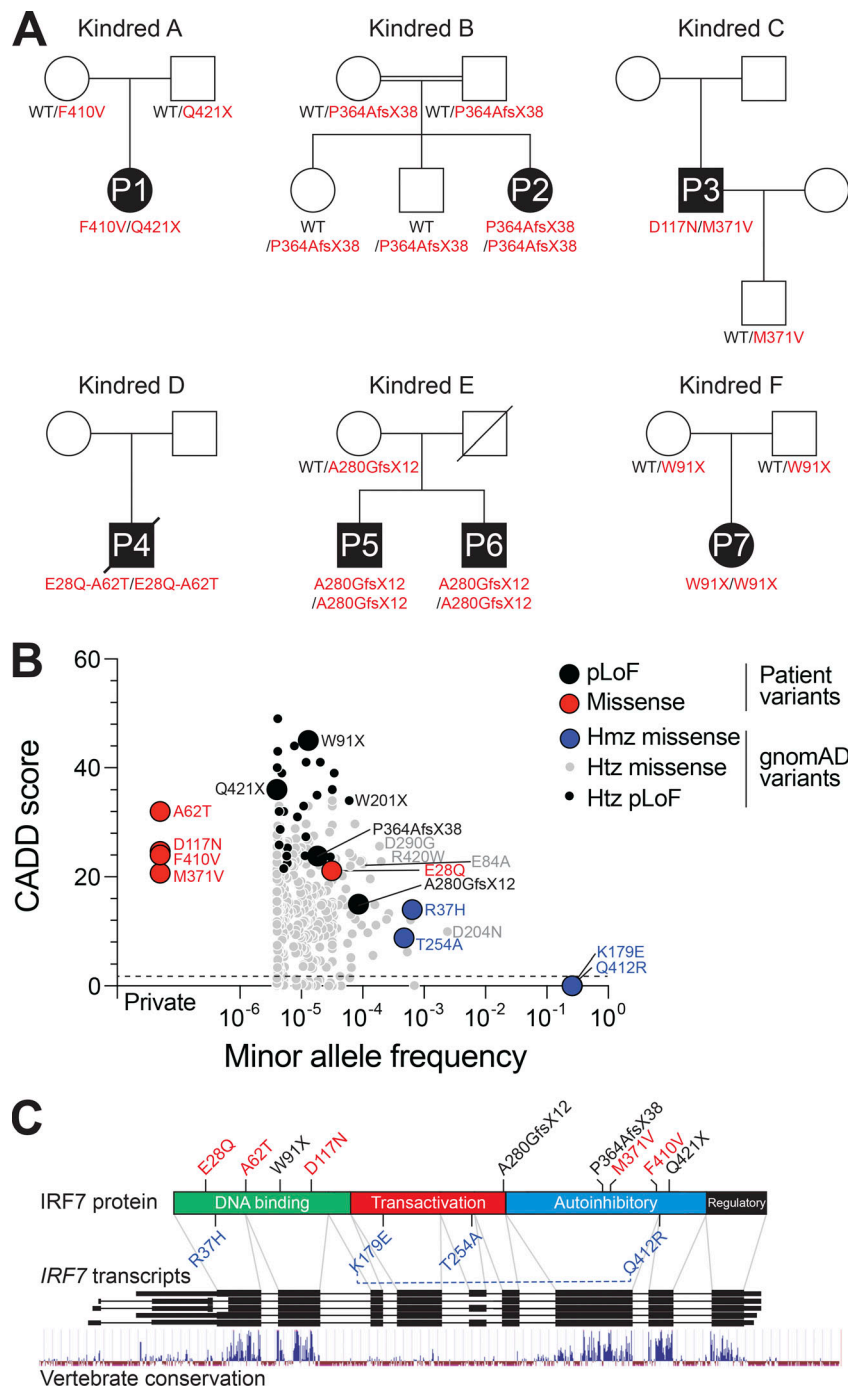


Figure 1. Patients with biallelic *IRF7* variants. (A) Pedigrees of the six kindreds containing seven patients with life-threatening viral infections (P1–P7) bearing rare biallelic *IRF7* variants. Solid black symbols indicate patients with critical viral infections. The *IRF7* genotype is indicated under each symbol. (B) The plot depicts the population frequency of *IRF7* missense and pLoF variants (gnomAD v2.1.1) against CADD score (v1.6, GRCh37). Symbols indicate a total of 463 variants, 4 identified exclusively in patients and 459 present in the gnomAD database. The patient-derived variants reported in this study are highlighted, with pLoF and missense variants colored black and red, respectively. The population-derived homozygous *IRF7* missense variants are highlighted in blue. (C) Schematic representation of *IRF7*. The lower part represents the genomic organization of the *IRF7* locus, with black rectangles indicating the exons of the gene according to different transcripts. Below, a track indicates vertebrate nucleotide conservation across the *IRF7* locus. The upper part shows the primary protein domain structure of *IRF7*. The N-terminal portion contains an α -helical DNA binding domain, followed by domains implicated in transactivation, autoinhibition, and regulation, as indicated. The positions of the patient-derived biallelic and population-derived homozygous *IRF7* variants are indicated. A blue dotted line indicates the linkage of the *IRF7* K179E and Q412R variants. Hmz, homozygous; Htz, heterozygous.

patient (P4) homozygous for combined *IRF7* (E28Q;A62T) variants and two patients (P5 and P6) homozygous for an *IRF7* A280GfsX12 variant presenting with critical and severe COVID-19, respectively. We also identified a patient (P7) homozygous for *IRF7* W91X in the cohort of patients with severe influenza. In total, we identified seven patients from six kindreds with life-threatening respiratory viral infections: five homozygotes and two compound heterozygotes. Cumulatively, we identified nine biallelic patient-associated *IRF7* variants (Fig. 1, A and B; and Table S1), five of which have previously been shown experimentally to be biochemically deleterious (Ciancanelli et al., 2015; Zhang et al., 2020). All of these *IRF7* variants had combined

annotation-dependent depletion (CADD) scores—a measurement of the deleteriousness of the variant used to prioritize causal variants in genetic analyses (Kircher et al., 2014)—greater than 10 and above the mutation significance cutoff (Itan et al., 2016).

Homozygous *IRF7* variants in public databases

We searched for nonsynonymous or splice site variants of *IRF7* present in the homozygous state in at least one individual reported in the public gnomAD database (v2.1.1, *IRF7* transcript ENST00000397574.2; Karczewski et al., 2020). Four missense variants were found: *IRF7* Q412R (global MAF = 0.26), K179E

(MAF = 0.26), R37H (MAF = 0.0006), and T254A (MAF = 0.0005; Table S1). *IRF7* Q412R and K179E were in complete linkage disequilibrium (D' and $r^2 = 1$) in all 1,000 Genomes populations. We therefore considered them to form a single allele, representing a common *IRF7* (Q412R;K179E) variant. For the 13 biallelic *IRF7* variants, including nine identified in patients, with the other four identified in gnomAD, we found that only two of the common gnomAD variants did not have CADD scores above the mutation significance cutoff (Fig. 1B and Table S1; Itan et al., 2016; Zhang et al., 2018). The 13 *IRF7* variants were located in different segments of the *IRF7* coding sequence. There were four nonsense variants predicted to be LoF (pLoF) and nine missense variants (Fig. 1C). Previous functional evaluations have shown the *IRF7* R37H and T254A variants to be neutral, whereas the *IRF7* F410V, Q421X, D117N, M371V, and P364AfsX38 variants were found to be deleterious (Ciancanelli et al., 2015; Zhang et al., 2020). No functional evaluations have been performed for the other six variants.

Population genetics of the *IRF7* gene

In addition to the four homozygous variants, there were 459 nonsynonymous coding and 13 splice donor or acceptor site variants of *IRF7* present in the heterozygous state in the gnomAD database (v2.1.1, *IRF7* transcript ENST00000397574.2). The nonsynonymous coding variants comprised 389 missense, 9 in-frame deletion or insertion, and 60 frameshift or stop-gain variants. The most common (MAF >0.01) missense variants were Q412R and K179E, and another 16 variants had a MAF >0.0001 (Table S1). Seven of these variants—*IRF7* R37H, R131Q, G214E, G247R, T254A, S285T, and R423P—were found to be neutral in functional tests (Ciancanelli et al., 2015; Zhang et al., 2020). Four of the *IRF7* variants that had not previously been tested—*IRF7* E84A, D290G, and R420W—had CADD scores >20 (CADD v1.6-GRCh37; Table S1), suggesting a likelihood of these variants being damaging and warranting functional investigations. The stop-gain, splice donor, or acceptor variants were all very rare (MAF <0.0001). The *IRF7* A280GfsX12 variant, found in the homozygous state in two patients with critical and severe COVID-19 (P5 and P6, respectively), was the most frequent *IRF7* pLoF variant in gnomAD (MAF = 0.00009). It is located in coding exon 6 of the gene and had a surprisingly low CADD score (10.1). *IRF7* exons 3–6 encode a transactivation domain that has been poorly conserved during evolution, contrasting with the other exons encoding the DNA-binding, autoinhibitory, and regulatory domains of the protein (Fig. 1C). Furthermore, exons 3, 5, 6, and 7 are symmetric, potentially facilitating the modular exclusion of exons 3–6 or of exon 6 alone, which would allow in-frame protein translation. The individuals heterozygous for the *IRF7* A280GfsX12 variant in gnomAD were predominantly of Swedish or Finnish ancestry (MAF 0.0007 and 0.0002, respectively). The high regional prevalence of this variant calls into question its putative deleteriousness and pathogenicity.

Expression and function of *IRF7* variants in vitro

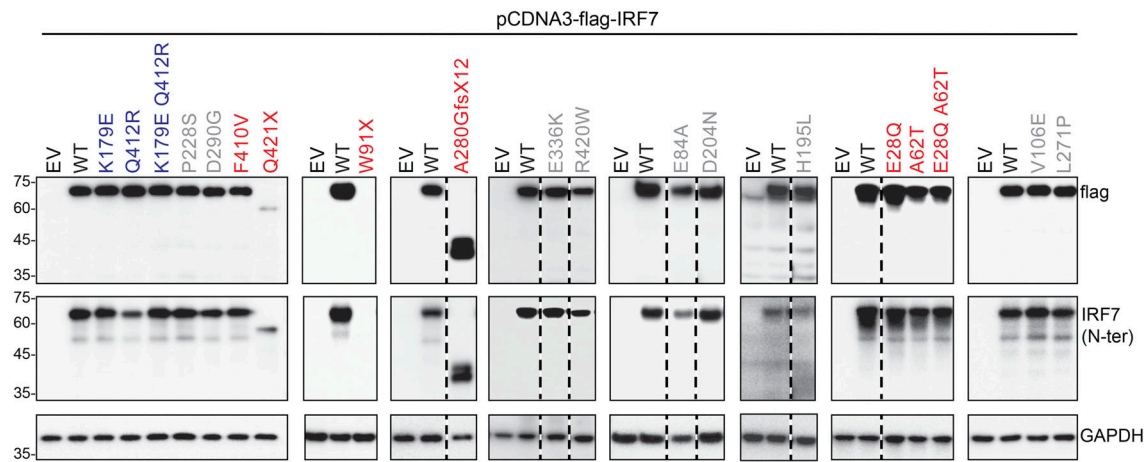
We first assessed the expression and function of the six newly discovered patient-derived *IRF7* variants and the four missense

IRF7 variants identified in a homozygous state in gnomAD. By transfecting HEK293T cells with plasmids encoding the different *IRF7* variants, we showed that the missense variants, including the combined (E28Q;A62T) and (K179E;Q412R) variants, were expressed normally (Fig. 2A). By comparison, the plasmids encoding A280GfsX12 and W91X yielded proteins of a lower molecular weight or resulted in a loss of expression, respectively. We assessed transcriptional activity by cotransfecting HEK293T cells with plasmids encoding the various *IRF7* variants and a luciferase reporter plasmid containing the regulatory sequence of *IFNB*, with or without Sendai virus infection, which induces type I IFN expression. The two previously reported *IRF7* LoF variants identified in P1, F410V and Q421X, served as controls. We found that *IRF7* E28Q had lower levels of activity than the WT *IRF7*, whereas *IRF7* A62T and the combined (E28Q;A62T) variants (as seen in P4) were completely defective (Fig. 2B). *IRF7* W91X (from P7) was LoF, consistent with the DNA-binding domain of *IRF7* being located at the N-terminus of the protein (aa 1–150). By contrast, *IRF7* A280GfsX12, from P5 and P6, was less active than *IRF7* WT protein, but activity was not completely absent. Interestingly, the two common variants, K179E and Q412R, displayed higher and lower levels of activity, respectively, than WT *IRF7*, when tested separately (Fig. 2B). As these two variants can be considered to constitute a single allele due to their strict linkage disequilibrium, we also tested their activity when combined into a single allele. Under these conditions, *IRF7* (K179E;Q412R) had normal activity, similar to that of WT *IRF7*. Thus, the three newly described homozygous *IRF7* variants in our four patients with severe respiratory viral infections are deleterious, whereas variants found in the homozygous state in the general population are neutral. Finally, we tested all additional variants identified in the heterozygous state in the general population with a MAF >0.0001, some of which had relatively high CADD scores (Table S1). *IRF7* D204N, P228S, and L271P were neutral, whereas E84A, V106E, D290G, E336K, and R420W had low levels of activity. *IRF7* H195L had higher levels of activity than the WT *IRF7*. Collectively, these results are consistent with *IRF7* being under moderate negative selection, like other genes underlying AR inborn errors of immunity (pLI = 0; consensus negative selection [CoNeS] = 0.212; supervised CoNeS [SCoNeS] = 0.858), with a cumulative pLoF = 0.001 (Rapaport et al., 2021).

IRF7 expression and function in patients' cells

We investigated the effect of the newly described *IRF7* variants in patients, by first assessing the induction of *IRF7* expression in peripheral blood mononuclear cells (PBMCs) stimulated with IFN- β . Samples were available from kindreds E (P6) and F (P7). Despite the production of *IRF7* fragments of lower molecular weight in ectopic expression systems of *IRF7* A280GfsX12 (Fig. 2A), we detected no *IRF7* in the cells of patients P6 or P7 after stimulation with IFN- β (Fig. 3A). We previously tested pDCs from two other *IRF7*-deficient patients and showed that *IRF7*-deficient pDCs could produce some IFN- β upon viral or TLR stimulation, but none of the other type I or III IFNs (Ciancanelli et al., 2015; Zhang et al., 2020). We evaluated *IRF7* activity in patients P5, P6, and P7 by stimulating PBMCs with TLR7

A



B

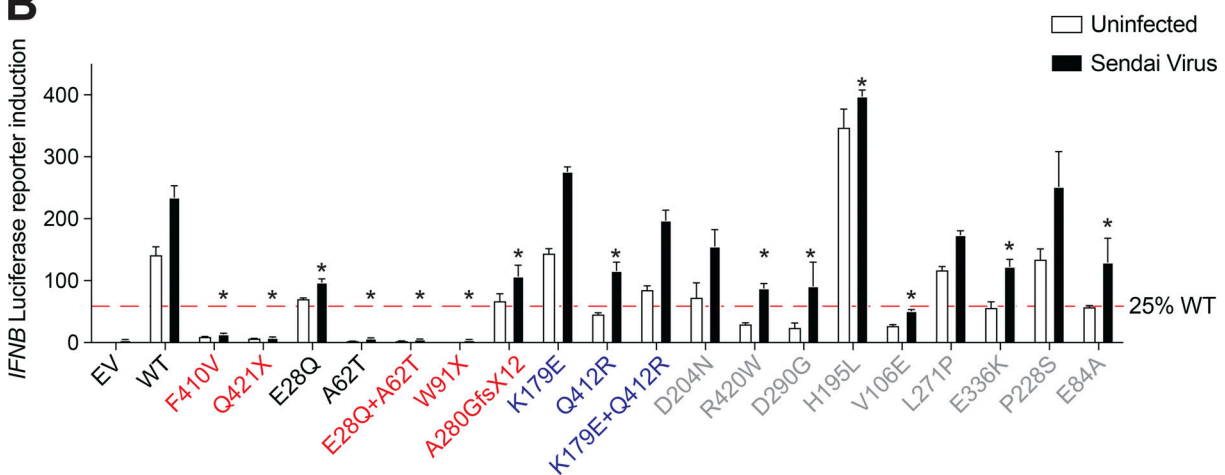


Figure 2. Expression and activity of novel *IRF7* variants. (A) HEK293T cells were transiently transfected with WT or mutant forms of *IRF7*. *IRF7* levels were assessed by Western blotting with antibodies against the N-terminus of *IRF7* or an N-terminal FLAG tag. GAPDH was used as a loading control. Representative immunoblots from at least three independent experiments are shown. EV, empty vector. (B) HEK293T cells were transiently transfected with WT or mutant forms of *IRF7*, together with an *IFN-β* luciferase reporter and a constitutively expressed reporter. Cells were either left untreated or infected with Sendai virus for 24 h before the assessment of normalized luciferase activity. The significance of differences between variants and the WT (mean ± SEM of $n \geq 3$ independent experiments) was determined by two-way ANOVA (*, $P < 0.05$). Source data are available for this figure: SourceData F2.

(imiquimod) or TLR9 (CpG oligodeoxynucleotide [ODN]) agonists, which are known to induce strong *IFN-α* and TNF production by pDCs (Cella et al., 1999; Reizis, 2019; Siegal et al., 1999). In patients P5 and P6, pDCs did not produce *IFN-α* in response to TLR7 or TLR9 agonists (Fig. 3, B and D). By contrast, the TLR agonists induced strong TNF production by pDCs, demonstrating a specific requirement of *IRF7* for the production of *IFN-α*, but not other proinflammatory cytokines, such as TNF. Both P5 and P6 had normal numbers of pDCs in peripheral blood, with 36 and 73 cells/μl of whole blood, respectively (healthy reference range: 12–178 cells/μl, median 64 cells/μl, $n = 38$). Similarly, pDCs from P7 did not produce *IFN-α* in response to TLR7 or TLR9 agonists (Fig. 3, C and E).

Of note, the transcriptional responses of P2 pDCs to SARS-CoV-2 and IAV infection were previously reported (Zhang et al., 2020). Further analyses of these data reveal that pDCs from P2 failed to respond to viral stimulation, in terms of the induction of type I and III *IFNs* transcripts, with the exception of *IFNB1*

mRNA that was weakly induced (Fig. S1). Patient PBMCs were also treated with the TLR3 agonist poly(I:C), which stimulates TNF expression by BDCA-3⁺ DCs (Jongbloed et al., 2010). No significant difference in TNF production following TLR3 stimulation was observed between the patients and healthy controls, as expected (Fig. S2). Overall, PBMCs from patients with homozygous *IRF7*-truncating W91X and A280GfsX12 variants had no *IRF7* protein and displayed defective *IFN-α* production by pDCs. The results of these physiological cellular assays thus indicate that the *IRF7* A280GfsX12 variant, which was hypomorphic when tested by overexpression in HEK-293T cells, is actually an LoF variant when constitutively expressed in pDCs, consistent with critical or severe COVID-19 pneumonia in both patients from kindred E (P5 and P6).

Clinical characteristics of *IRF7*-deficient patients

All patients with biallelic *IRF7* LoF variants presented clinically with severe viral respiratory infections (Table 1). The patients

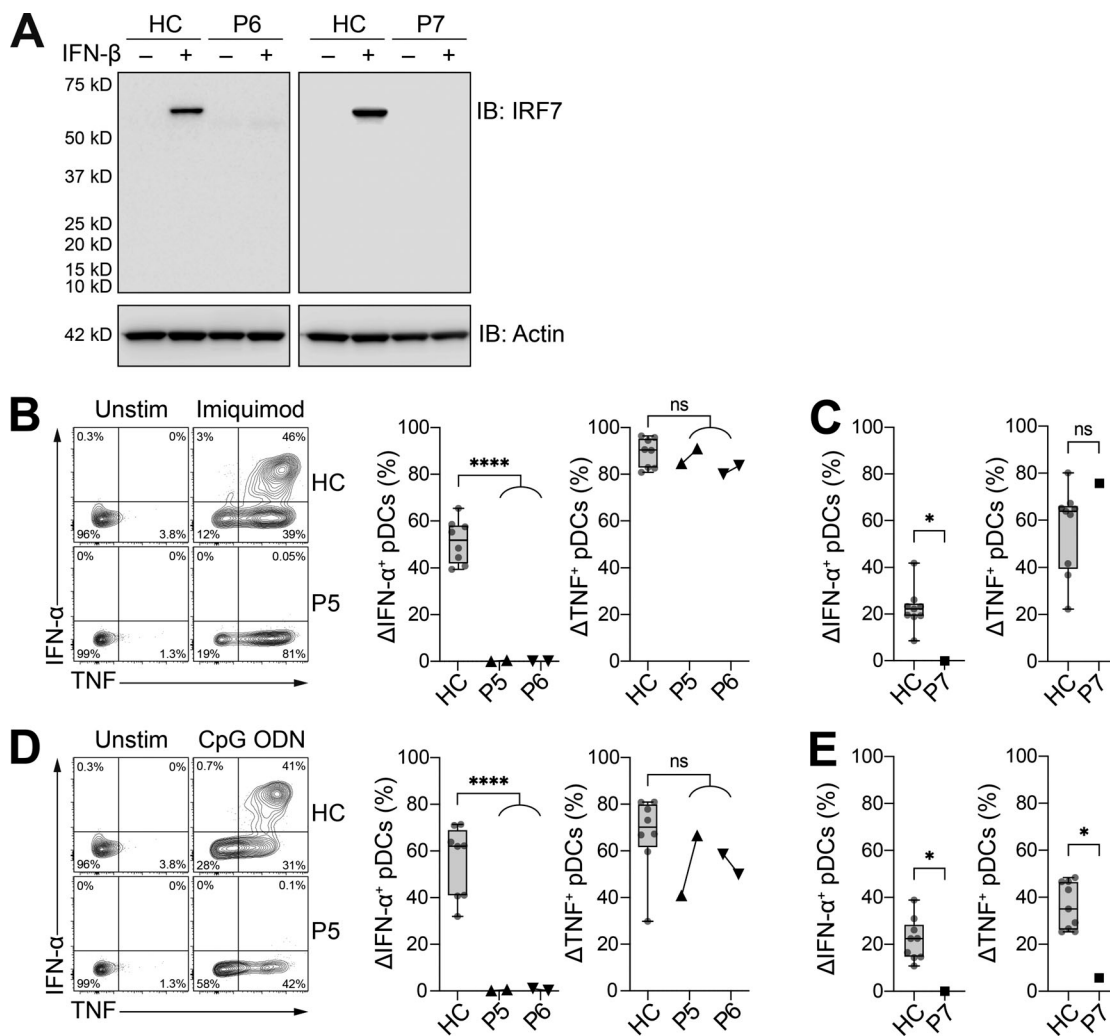


Figure 3. Patients with the newly discovered *IRF7* variants do not produce IRF7 protein or IFN-α upon pDC stimulation. (A) Protein levels for IRF7 in PBMCs with and without IFN-β stimulation for 24 h; comparison of patients and healthy controls (HC). Actin staining was used as a loading control. Representative immunoblots (IB) from single independent experiments per patient are shown. (B and C) Frequency of IFN-α⁺ and TNF-producing pDCs (live Lin⁺CD11c⁺HLA-DR⁺CD303⁺CD123⁺) after 6 h of stimulation with imiquimod for fresh (B) and thawed (C) PBMCs. (D and E) Frequency of IFN-α⁺ and TNF-producing pDCs (live Lin⁺CD11c⁺HLA-DR⁺CD303⁺CD123⁺) after 6 h of stimulation with CpG ODN for fresh (D) and thawed (E) PBMCs. For P5 and P6, cells were assessed at two independent time points 6 mo apart. (A–E) All data are presented as the frequency of responding cells minus the frequency of the corresponding unstimulated controls. Box plots are bound by the 25th and 75th percentiles. The median is marked, and the whiskers indicate the minimum and maximum. Individual values are plotted. Unpaired *t* tests were performed to compare healthy controls (HC; *n* = 8–9) with patients. *, *P* < 0.05; ****, *P* < 0.0001. Source data are available for this figure: SourceData F3.

originated from five different countries: France (P1), Italy/Belgium (P2), Turkey (P3), Iran (P4), Sweden (P5 and P6), and Belgium (P7). Detailed descriptions of the clinical presentations of P4–P7 are provided in the supplementary material, with an update of the clinical presentations of the previously reported P1–P3. Age at clinical presentation ranged from 6 mo to 50 yr. Patients were healthy before presenting with severe infections with respiratory viruses: IAV (P1 and P6), SARS-CoV-2 (P2–P5), and respiratory syncytial virus (RSV; P7), all of which are single-stranded RNA viruses. Five patients were hospitalized for a single severe viral infection, whereas two suffered multiple severe viral infections. Patient P6 was initially hospitalized with IAV infection in adolescence before requiring oxygen treatment for severe COVID-19 in 2020, and patient P7 first presented with

RSV at 6 mo of age and has since been treated for severe, consecutive IAV and adenovirus infections. Prophylactic measures, such as annual influenza vaccination (P1 since 2014; P5, P6, and P7 since 2021) and COVID-19 vaccination (P1, P2, P3, P5, P6, and P7 in 2021), were implemented after molecular diagnosis.

Adaptive antiviral T cell immunity in IRF7-deficient patients

T cell responses are a hallmark of adaptive immunity to viral infections (Bradley and Thomas, 2019). We therefore quantified memory T cell responses in patients P5 and P6 in response to stimulation with peptides from a range of common viruses. The IFN-γ responses of the patients' cells were similar to those of healthy controls following stimulation with peptides from human herpesviruses, human cytomegalovirus (HCMV) and EBV

Table 1. Genetic, demographic, and clinical features of IRF7-deficient patients

Feature	P1	P2	P3	P4	P5	P6	P7
IRF7 variants (NM_001572)	p.(Phe410Val); p.(Gln421Ter)	p.(Pro364AlafsX38); p.(Pro364AlafsX38)	p.(Asp117Asn); p.(Met371Val)	p.(Glu28Gln; Ala62Thr); p.(Glu28Gln; Ala62Thr)	p.(Ala280GlyfsX12); p.(Ala280GlyfsX12)	p.(Ala280GlyfsX12); p.(Ala280GlyfsX12)	p.(Trp91Ter); p.(Trp91Ter)
Age at onset	2.5 yr	49 yr	50 yr	29 yr	38 yr	31 yr	6 mo
Ancestry (Residence)	France	Italy (Belgium)	Turkey	Iran	Sweden/Finland (Sweden)	Sweden/Finland (Sweden)	Belgium
Viral susceptibility	Influenza	SARS-CoV-2	SARS-CoV-2	SARS-CoV-2	SARS-CoV-2	Influenza; SARS-CoV-2; TBE virus	RSV; influenza; adenovirus
BMI (kg/m²)		30.0	27.3	29.4	23.4	22.0	
Risk factors		Obesity	None		None	None	
Outcome	Alive and well at age 14 yr	Alive and well at age 50 yr	Alive and well at age 51 yr	Died from COVID-19 at age 29 yr	Alive and well at age 39 yr	Alive and well at age 32 yr	Alive and well at age 5 yr
Vaccinations	Influenza since 2014; COVID-19 since 2021			Not applicable	Influenza since 2021; COVID-19 since 2021	Influenza since 2021; COVID-19 since 2021	Influenza since 2021; COVID-19 since 2021
Reference	Ciancanelli et al., 2016	Zhang et al., 2020	Zhang et al., 2020				

(Fig. 4, A and B). Interestingly, both patients had significantly higher frequencies of memory CD4⁺ T cells responding to three of the five IAV peptides tested (MP1, NA, and NP) than the controls (Fig. 4 A). Furthermore, the patients had significantly higher frequencies of SARS-CoV-2-responding CD4⁺ and CD8⁺ memory T cells than healthy donors, including individuals with a history of mild COVID-19. Both patients were hospitalized for COVID-19, but only P6 had previously suffered from severe influenza, despite both P5 and P6 having high frequencies of IAV-specific CD4⁺ memory T cells. Notably, the analyzed samples were collected from the patients before vaccination against influenza and COVID-19. We also analyzed T cell responses in patients P5 and P6 after the stimulation of whole blood with influenza inactivated split-virus vaccine or whole inactivated SARS-CoV-2 virus, quantifying T cell blasts after 6 d of stimulation. Consistent with the frequency of CD4⁺ memory T cells responding to IAV peptides (Fig. 4 A), P5 and P6 had significantly stronger CD4⁺ T cell blast responses to influenza virus vaccine stimulation than healthy controls (Fig. S3 A). In response to SARS-CoV-2, both P5 and P6 had CD4⁺ and CD8⁺ T cell responses within the range observed for healthy controls convalescing from COVID-19 (Fig. S3 B).

Adaptive antiviral B cell immunity in IRF7-deficient patients

We assessed the humoral responses to viruses by investigating the exposure of the patients to viruses with VirScan (Xu et al., 2015). Samples were collected from the patients before vaccination against influenza and COVID-19. We found that the patients were seropositive for pathogens commonly found in age-matched controls, showing that they were able to control most common pathogens, including rhinoviruses, herpesviruses, enteroviruses, *Streptococcus pneumoniae*, and *Mycoplasma pneumoniae* (Fig. S3 C). In analyses focusing on antigens specific

to IAV, P1 and P3 were seropositive for the IAV nonstructural 1 (NS1) protein (Fig. S3 D). In analyses focusing on antigens specific to coronaviruses, P1, P2, P3, and P6 were seropositive for SARS-CoV-2, reflecting their known history of COVID-19 (P2, P3, and P6) and vaccination (P1). Surprisingly, P5 was seronegative for all four SARS-CoV-2 spike protein-specific antigens. P1 and P6 were also seropositive for antigens specific to common coronaviruses, such as 229E and NL63, suggesting that they were able to control less virulent coronaviruses (Fig. S3 E). In patients P5 and P6, we confirmed by classic serology that both patients had mounted antibody responses to EBV, HSV, measles virus, mumps virus, and rubella virus. Patients P1 and P7, who did not present with clinical COVID-19, have been vaccinated with three and two doses, respectively, of the BNT162b2 mRNA vaccine. P1 responded by producing antibodies against the SARS-CoV-2 spike protein, as demonstrated by the VirScan analysis (Fig. S3 E). P7 also developed antibodies against the spike protein after vaccination (anti-S IgG level 1 mo after the second dose: 20,195 AU/ml [cutoff > 5 AU/ml]). Thus, IRF7-deficient patients can mount robust adaptive responses to viruses and to mRNA vaccines, providing protection against severe infections. Moreover, these patients were found to have been infected with a wide range of common viruses, which they controlled normally.

Impaired type I and III IFN expression in IRF7 deficiency predisposes to severe respiratory viral infections

Altogether, we report inherited IRF7 deficiency in seven patients from six kindreds in five countries. All nine alleles were hypomorphic when tested by overexpression in HEK293T cells (Fig. 2 B; Ciancanelli et al., 2015; Zhang et al., 2020); however, in primary cells from siblings P5 and P6, as well as P7, homozygous expression of two of the alleles conferred a complete functional

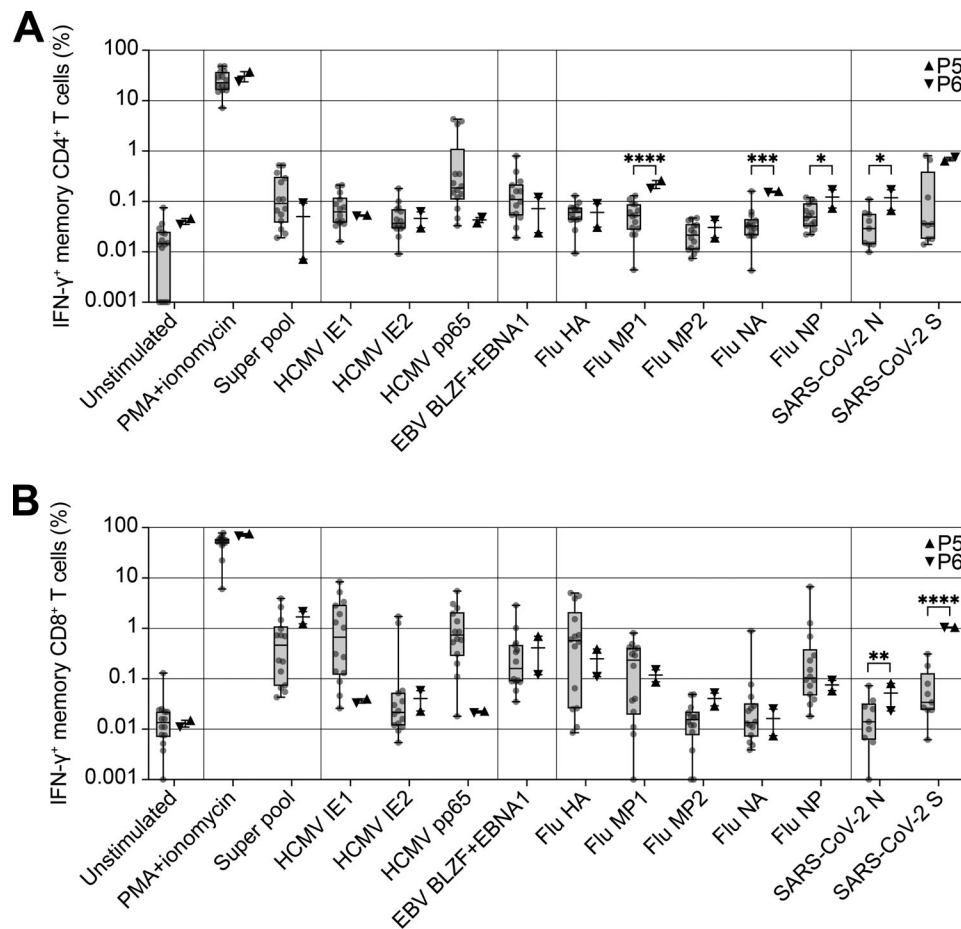


Figure 4. IRF7-deficient patients have enhanced CD4⁺ T cell responses to influenza and coronaviruses. (A and B) Frequency of IFN- γ -producing memory CD4⁺ (live Lin⁺CD3⁺CD4⁺CD8⁺CCR7⁺CD95⁺; A) or CD8⁺ (live Lin⁺CD3⁺CD8⁺CD4⁺CCR7⁺CD95⁺; B) T cells after stimulation with peptides or PMA + ionomycin for 6 h. Unstimulated controls are shown on the left of the graph. Box plots are bound by the 25th and 75th percentiles. The median is marked, and the whiskers indicate the maximum and minimum. Individual values are plotted. Unpaired *t* tests were performed to compare healthy controls (HC; *n* = 9–14) and patients (P5 and P6). *, *P* < 0.05; **, *P* < 0.01; ***, *P* < 0.001; ****, *P* < 0.0001.

defect. The patients from all six families thus suffer from a complete form of AR deficiency. Inherited IRF7 deficiency underlies at least four unusually severe respiratory viral infections, with influenza and COVID-19 being the most common and severe (Ciancanelli et al., 2016; Zhang et al., 2022). The mechanism of viral pneumonia in patients with IRF7 deficiency probably involves the disruption of type I and III IFNs in both pDCs and respiratory epithelial cells (Ciancanelli et al., 2015; Zhang et al., 2020), illustrated by undetectable blood IFN- α levels during COVID-19 infection (Zhang et al., 2020). Patients with TLR3 deficiency are prone to both influenza and COVID-19 pneumonia, perhaps because TLR3 regulates the basal type I IFN levels in respiratory epithelial cells, as it does in fibroblasts and cortical neurons (Gao et al., 2021; Lim et al., 2019; Zhang et al., 2020; Zhang et al., 2007). By contrast, patients with TLR7 deficiency have defective pDCs and seem to be normally resistant to influenza but highly vulnerable to COVID-19 (Asano et al., 2021). IRF7 deficiency affects both pDCs and epithelial cells and both type I and III IFNs. The intact type III IFN activity in IFNAR1-deficient patients with critical COVID-19 pneumonia suggests that the poor induction of type I IFN impairs host defense

against SARS-CoV-2 in the respiratory tract of IRF7-deficient patients (Zhang et al., 2020). By contrast, critical influenza has been reported in only two of the 25 patients with IFNAR1 or IFNAR2 deficiency, suggesting that type III IFN may help to protect against influenza in most cases, accounting for the occurrence of critical influenza in IRF7-deficient patients, who have impaired production of both type I and III IFNs (Abolhassani et al., 2022; Bastard et al., 2022; Bastard et al., 2021; Duncan et al., 2015; Duncan et al., 2022; Gothe et al., 2020; Hernandez et al., 2019; Zhang et al., 2020).

Variable disease penetrance in IRF7 deficiency

Penetrance is incomplete in IRF7-deficient patients, at least for RSV, adenovirus, and influenza, although we cannot be sure that the same serotypes infected other IRF7-deficient individuals. There is probably higher penetrance for COVID-19, as indicated by the two brothers (P5 and P6) manifesting life-threatening SARS-CoV-2 infection. Only one of the brothers presented clinically with influenza, but both had high influenza antibody titers and T cell responses indicative of prior infection. Most SARS-CoV-2 strains are more virulent and induce production of

smaller amounts of type I IFN than seasonal influenza viruses (Blanco-Melo et al., 2020; Chu et al., 2020). The follow-up of existing IRF7-deficient patients and the molecular diagnosis of additional patients with this deficiency should shed further light on the clinical infectious disease spectrum and penetrance of IRF7 deficiency and the role of IRF7 in other noninfectious diseases (Bidwell et al., 2012; Zhao et al., 2017). *Irf7* knockout mice could be studied to provide more insight into the molecular and cellular basis of disease in IRF7-deficient patients, particular as such mice have a susceptibility to viral infections somewhat comparable to that of IRF7-deficient patients (Ciancanelli et al., 2016; Hatesuer et al., 2017). However, it is difficult to model natural human infections in inbred mice, because of the experimental nature of the infections in mice (Casanova and Abel, 2021). The combination of such studies with the use of induced pluripotent stem cell-derived pDCs and respiratory epithelial cells to model these infections in human cells could potentially elucidate some of the compensatory pathways reducing infectious disease penetrance (Sontag et al., 2017).

Narrow spectrum of viral susceptibility in IRF7 deficiency compared with other type I IFN deficiencies

It is also surprising that IRF7-deficient patients are not prone to other viral infections repeatedly seen in many of the 25 patients with IFNAR1 or IFNAR2 deficiency reported to date, such as disseminated disease following MMR or YFV-17D vaccination and HSV-1 encephalitis (Abolhassani et al., 2022; Bastard et al., 2022; Bastard et al., 2021; Duncan et al., 2015; Duncan et al., 2022; Gothe et al., 2020; Hernandez et al., 2019). These viral susceptibilities, and predisposition to severe disease from additional human herpesviruses, are also common to patients with other core deficiencies of the type I IFN response, such as STAT1, STAT2, and IRF9 deficiencies (Duncan et al., 2021; Meyts and Casanova, 2021). These patients also have viral susceptibility profiles similar in some respects to those of IRF7-deficient patients, with select cases of severe disease caused by influenza viruses, RSV, and adenoviruses (Alosaimi et al., 2019; Hernandez et al., 2018; Le Voyer et al., 2021). However, it is striking that the IRF7-deficient patients have tolerated live-attenuated vaccines and so many common viruses, particularly those infecting tissues outside the respiratory tract. This finding also contrasts with those for *Irf7* knockout mice and in vitro studies with human IRF7-deficient cells, which have reported susceptibility to a broader range of viral infections (Hatesuer et al., 2017; Honda et al., 2005). Furthermore, pDCs from IRF7-deficient patients lack induction of type I and III IFNs, with the exception of IFN- β , whose induction was impaired but not abolished (Fig. S1; Ciancanelli et al., 2015; Zhang et al., 2020).

So, how can we account for the relatively narrow and pulmonary clinical phenotype of IRF7 deficiency relative to other type I IFN deficiencies (e.g., IFNAR1 deficiency)? A first hypothesis is that IFN- β may be involved, providing sufficient immunity to viruses in various tissues and organs. This would imply that IFN- β is insufficient to handle some respiratory viruses, at least in certain settings (a particularly virulent influenza strain, SARS-CoV-2, or a large inoculum of RSV or

adenovirus). The lack of severe infections in IRF7-deficient patients after vaccination with live attenuated vaccines, especially MMR, which can cause severe infections in patients with deficiencies of STAT1, STAT2, IFNAR1, and IFNAR2, suggests that the amplification of type I IFN signaling mediated by IRF7 may be dispensable if the attenuated strains trigger stronger type I IFN responses than the WT virus (Poyhonen et al., 2019; Shingai et al., 2007). Furthermore, the patients' narrow viral susceptibility may reflect the variable ways different viruses interact with human cells. Herpesviruses, for example—which were controlled normally by all IRF7-deficient patients—employ multiple immune evasion strategies to reduce type I IFN responses and establish latency (Garcia-Sastre, 2017; Hoffmann et al., 2015; Weekes et al., 2014). Conceivably, this process might limit the requirement for type I IFNs in the control of chronic herpesvirus infections.

Alternatively, or additionally, the patients' myeloid and lymphoid cells may ensure more robust innate immunity than in patients with type I IFN receptor and signaling deficiencies. Our data suggest that IRF7-deficient patients can have particularly strong adaptive immunity to viruses. We show here that they have a robust CD4⁺ T cell response to IAV and SARS-CoV-2 (Fig. 4). Type I IFN has been implicated in both the promotion and limitation of T cell responses, the precise balance being determined by the timing of type I IFN exposure relative to T cell activation (Crouse et al., 2015). Low type I IFN levels, particularly in the bloodstream, may limit the natural killer cell-mediated killing of virus-specific T cells, thereby facilitating the establishment of larger memory T cell pools (Crouse et al., 2014). Established T cell responses may at least partly account for the absence of viral disease recurrence in these patients, at least at the time of reporting, even for respiratory tract infections, in particular SARS-CoV-2, which is likely the most virulent virus to have infected these patients.

In conclusion, characterization of the IRF7-deficient individuals identified to date suggests a relatively narrow susceptibility to critical infections with respiratory viruses, with some individuals displaying strong adaptive responses that may protect them against severe viral disease for decades. Residual IFN- β immunity might also contribute to host defense against viruses. Vaccination against common viral pathogens, including SARS-CoV-2, appears to be an effective intervention that can protect these patients from infectious disease.

Materials and methods

Patients

Samples were obtained from the probands, parents, and relatives, with written informed consent. The study was approved by the Swedish Ethical Review Authority (CovPID: 2020-01911), the Ethics Committee UZ Leuven (BIOKID: S63807), the Ethics Committee of Hôpital Erasme (P2020-203), the French Ethics Committee “Comité de Protection des Personnes,” the French National Agency for Medicine and Health Product Safety, the “Institut National de la Santé et de la Recherche Médicale,” in Paris, France (protocol no. C10-13); and the Rockefeller

University Institutional Review Board in New York, NY (protocol no. JCA-0700).

Case reports

Kindred A

The clinical presentation and progression of patient P1 have been described in detail elsewhere (Ciancanelli et al., 2015). Patient P1 has been vaccinated against influenza annually since 2014, with one or two doses, depending on the results of post-vaccination serologic tests. She was also vaccinated with three doses of the COVID-19 BNT162b2 mRNA vaccine (Pfizer) in 2021. She has suffered no severe infections since 2011 and remains EBV seronegative.

Kindred B

Patient P2 is a Belgian woman born in 1971 to first-cousin parents of Italian origin. In March 2020, she presented with a flu syndrome, including fatigue, fever (39°C), nausea and vomiting, myalgia, and headache. She had no history of contact with a confirmed COVID-19 case, but her brother had developed flu-like symptoms lasting a few days in the previous week. Upon hospital admission 1 wk after onset, she was diagnosed with COVID-19 based on clinical presentation: fever, crackles on auscultation, dyspnea and hypoxemia (arterial oxygen saturation of 93% despite 6 liter/min oxygen support), a typical computerized tomography (CT) scan with bilateral basal condensation and widespread ground-glass opacities, and blood test results suggestive of an inflammatory syndrome (white blood cells: 13,680/mm³ with 84.5% polynuclear neutrophils, 11.3% lymphocytes, and 4.1% monocytes; C-reactive peptide [CRP]: 450 ng/liter). She also had high transaminase (aspartate aminotransferase: 53 IU/liter, alanine aminotransferase: 51 IU/liter) and γ -glutamyl transferase (157 IU/liter) levels. COVID-19 was confirmed by a positive SARS-CoV-2 PCR test on a nasopharyngeal swab, with negative results for IAV and IBV antigens.

The patient rapidly developed acute respiratory distress syndrome. She was admitted to the intensive care unit (ICU), intubated, placed on assisted ventilation, and treated with hydroxychloroquine and amoxicillin/clavulanic acid for 4 d. She was then shifted onto piperacillin/tazobactam and vancomycin. 1 wk after admission, her condition worsened owing to asthma exacerbation, and she suffered from hypoxemia and hypercapnia despite assisted ventilation. She was transferred to Hôpital Erasme for extracorporeal membrane oxygenation, which was maintained for 4 d. She was treated with hydroxychloroquine, lopinavir/ritonavir, piperacillin/tazobactam, corticosteroids, and bronchodilators. She developed subglottic edema, necessitating tracheostomy. Bacteriological analysis of bronchoalveolar lavage revealed superinfection with *Escherichia coli* and *Staphylococcus aureus* (cytology: leukocytes, alveolar macrophages, bronchial cells). The patient also developed a urinary tract infection with *E. coli*, for which she was treated with oxacillin for 10 d. She also carried multidrug-resistant *Enterococcus faecium*.

Progressive weaning from ventilation was initiated after 10 d on extracorporeal membrane oxygenation, and the tracheostomy was removed 10 d later. The patient was transferred to the pulmonology

ward and discharged 6 wk after admission. She was still extremely malnourished and debilitated, requiring daily physiotherapy.

Relevant blood test results are as follows: blood type O+, maximum concentrations of 47 pg/ml for IL-6, 14,808 ng/ml for D-dimers, and 160 ng/liter for CRP. Persistent hepatic cytolysis and cholestasis were observed during the patient's ICU stay. SARS-CoV-2 PCR remained positive until 1 wk before discharge. White blood cell count in remission: 8,700/mm³, with 44.5% neutrophils and 46.4% lymphocytes.

The patient had had asthma since the age of 30 yr, treated with inhaled ipratropium bromide and beclomethasone. She was overweight (body mass index [BMI] 30 kg/m²), with type 2 diabetes treated with metformin and tachycardia episodes treated with bisoprolol. Previous medical history included surgery for carpal tunnel syndrome and traumatic brain injury (with the fortuitous discovery of benign brain lesions).

The patient's previous infectious history is as follows: The patient described recurrent infections since childhood. She underwent tonsillectomy at ~9 yr of age and subsequently suffered four to five episodes of sinusitis and/or otitis per year until adulthood. These infections were considered viral, and therefore she rarely received antibiotics. She had four flu episodes, twice as a teenager and twice as an adult, with 7–10 d of high fever, fatigue, nausea and vomiting, myalgia, and dizziness. She had never been vaccinated against influenza. She had bronchitis with asthma exacerbation every year until a few years ago but had never had to be hospitalized. She developed hepatitis (digestive symptoms and icterus) in childhood, together with her siblings. She recalls suffering from mumps, varicella, and measles as a child, as well as numerous other infectious episodes.

She had not been vaccinated with *Bacillus Calmette–Guérin*. She received a preconception recall rubella vaccine and had anti-rubella IgG. Blood tests also revealed CMV exposure, with a normal IgG response.

The patient's father is diabetic and has a heart condition. She has a sister living with the parents who has suffered from depression and underwent tonsillectomy. Her brother also underwent tonsillectomy and is in good health. The patient has three healthy daughters, aged 18, 22, and 26 yr.

Kindred C

Patient P3 is a Turkish man born in 1960 who contracted COVID-19 in April 2020. He was hospitalized and admitted to the ICU. He presented with flu-like symptoms, including cough, dyspnea, fever, headache, and myalgia. His chest x ray indicated severe pneumonia and ground-glass opacities, consistent with COVID-19. On admission, he had a peripheral capillary oxygen saturation (SpO₂) of 84% with oxygen support. He received 7 liters oxygen/min to keep his SpO₂ at 78–84%. The patient was initially prescribed hydroxychloroquine and azithromycin. On day 3 of hospitalization, his body temperature increased to 39°C. Favipravir was added to the regimen, followed by tocilizumab. Tocilizumab was administered for 2 d and then stopped. Favipravir was stopped on day 5, and the fever subsided on the third day of treatment. The need for oxygen supplementation eventually subsided, and the patient was monitored, without oxygen,

for 15 d after admission. He was discharged from the hospital after 17 d. He has BMI of 27.3 kg/m², does not smoke, and has no comorbidities (no asthma, recurrent infections, immunodeficiency, or hypogammaglobulinemia).

Kindred D

Patient P4, an Iranian man born in 1991, presented with flu-like symptoms, including cough, fever, and dyspnea of 7 d duration before admission. PCR on a nasopharyngeal sample was positive for SARS-CoV-2. Upon admission, the patient had a SpO₂ of 60% and was intubated in the emergency ward. He was admitted to the ICU, where he was placed on mechanical ventilation. He received IFN- β 1a (initiated at admission, 24 million IU equivalent, three doses), methylprednisolone (40 mg/d), and hemoperfusion. He died 20 d after admission. He had an unremarkable medical history, a BMI of 29.4 kg/m², did not smoke, and had no comorbid conditions other than being overweight (no asthma, recurrent infections, immunodeficiency, or hypogammaglobulinemia).

Kindred E

Patients P5 and P6, two brothers of Swedish/Finnish ethnic origin, born in 1982 and 1989, respectively, suffered from critical/severe SARS-CoV-2 infections during the first wave of the COVID-19 pandemic in Stockholm, Sweden, in the spring of 2020.

The elder brother (P5) was previously healthy, with no significant infection episodes. As a child, he was vaccinated in accordance with the Swedish vaccination program, which includes live MMR vaccines. In March 2020, he developed dyspnea, cough, fever, chest pain, impaired smell and taste, diarrhea, fatigue, and muscle and joint pain. Contact tracing suggested that he was infected by a colleague who had recently visited Austria. 10 d after the onset of symptoms, he was admitted to the infectious disease clinic at a tertiary hospital. A PCR test for SARS-CoV-2 was positive, as subsequently confirmed by a positive serological test for IgG anti-spike receptor-binding domain antibodies. Laboratory tests at admission showed high CRP levels (402 mg/liter), a high leukocyte count (11.6×10^9 /liter, including 9.7×10^9 neutrophils/liter), and lymphopenia (0.6×10^9 /liter). Chest x ray showed pronounced bilateral pulmonary opacification, predominantly in the lower lobes. Patient P5 suffered respiratory failure and was transferred to the ICU after 2 d. He required intubation with assisted ventilation for 5 d. He spent 15 d in the ICU before returning to the infectious disease clinic. During hospitalization, he received chloroquine phosphate and antibiotics (erythromycin, cefotaxime, ceftriaxone, meropenem), but no concomitant bacterial infections were detected. He was discharged home after 23 d in hospital.

3 wk after discharge, he sought medical assistance for heart palpitations. Transient myocardial damage was suspected; exercise electrocardiogram and troponin levels were normal on follow-up. He suffered from mild dyspnea, mild fatigue, and body aches for a few months but, with the exception of mild fatigue, he had almost fully recovered 6 mo after admission and had returned to work full-time. Laboratory tests performed 7 mo after admission showed normal counts of leukocytes (4.5×10^9 /liter), neutrophils (2.6×10^9 /liter), and total lymphocytes ($1,500 \times 10^6$ /liter). Immunoglobulin analyses were normal, with 0.97 g/

liter IgM, 11.1 g/liter IgG, and 4.1 g/liter IgA. No autoantibodies against IFN- α 2 were detected.

The younger brother of patient P5 (P6) had had recurrent ear infections during his early school years, requiring the insertion of a tympanostomy tube. He had also been vaccinated according to the Swedish vaccination program for children. During his teenage years, he suffered from two severe infectious episodes: one influenza episode requiring hospitalization at the age of 14 yr, and one streptococcal infection requiring hospitalization and antibiotic treatment. In the middle of April 2020, he developed dyspnea, fever, muscle pain, and a sore throat. 7 d later, he was admitted to the infectious disease clinic of a tertiary university hospital. A PCR test for SARS-CoV-2 was positive and was subsequently confirmed by a positive serological test for IgG anti-spike receptor-binding domain antibodies. Laboratory tests performed on admission showed high CRP levels (306 mg/liter), a high leukocyte count (11.6×10^9 /liter, including 7.2×10^9 neutrophils/liter), and lymphopenia (0.6×10^9 /liter). IL-6 levels were 7.7 ng/liter and procalcitonin levels were 0.63 μ g/liter. The patient's body temperature reached 41.5°C. Oxygen treatment was sufficient to maintain adequate blood oxygen saturation and intubation was never needed. Tocilizumab treatment was considered, but never administered, after rapid improvement on day 4 of hospitalization. A chest CT scan showed pronounced bilateral pulmonary opacification that was predominantly peripheral and in the lower lobes, more pronounced on the left side. No pulmonary embolism was detected. The patient received cefotaxime and ceftriaxone, but no concomitant bacterial infections were found. The patient was discharged home after 4 d of hospitalization and was able to return to work after 10 d of sick leave.

8 mo after admission, he continued to feel a slight loss of stamina but had otherwise fully recovered. Laboratory tests results were normal (5.3×10^9 /liter leukocytes, 3.7×10^9 /liter neutrophils, and 1.300×10^9 /liter total lymphocytes). Immunoglobulin analyses showed IgM levels (0.43 g/liter) and IgG levels (9.7 g/liter) to be normal and IgA levels (4.6 g/liter) to be slightly high. No autoantibodies against IFN- α 2 were detected.

In the middle of August 2021, patient P6 developed a severe headache with fever. After 4 d, a sudden improvement was observed that lasted 2 d before the symptoms worsened again. 9 d after the onset of the initial symptoms, patient P6 developed diplopia and was admitted to the infectious disease clinic at a tertiary university hospital. He had no signs of respiratory infection or cognitive impairment. During the weeks before he developed symptoms, patient P6 had been on vacation in the Stockholm archipelago, where he had received several tick bites. He had received his third dose of tick-borne encephalitis (TBE) vaccine 1 mo before the onset of symptoms. On admission, he had a CRP concentration of 10 mg/liter, a high leukocyte count (10.8×10^9 /liter including 8.3×10^9 neutrophils/liter), and a normal lymphocyte count (1.6×10^9 /liter). Cerebrospinal fluid (CSF) analyses revealed pleocytosis, with a high leukocyte count (248×10^6 /liter, including 226×10^6 monocytes/liter), and an albumin concentration of 745 mg/liter. Serological tests on blood and CSF (IgG and IgM) were negative for *Borrelia burgdorferi*.

Serous meningitis was suspected. PCR for the TBE virus was negative on CSF, but serological tests were positive on both CSF and serum, with high titers of neutralizing antibodies in the serum, suggesting a breakthrough infection despite three doses of vaccine. After 2 d in hospital, the patient's symptoms improved rapidly; he was discharged home after 3 d and recovered fully.

Kindred F

Patient P7 is a Belgian girl born at term in 2016, after an uneventful pregnancy, with a birth weight of 3,570 g and an Apgar score of 9/10. The parents are not known to be consanguineous. At the age of 6 mo, she was admitted to hospital with PCR-proven RSV bronchiolitis, clinically diagnosed on the basis of bilateral wheezing and crackles, complicated by suspected bacterial pneumonia, with bilateral patchy infiltrates on x ray, responding to antibiotic treatment. At the age of 7 mo, patient P7 was hospitalized with IAV bronchopneumonia and a high fever and given oxygen therapy and antibiotic treatment. At the age of 8 mo, she was admitted for sepsis and metabolic acidosis. All cultures (blood, urine, CSF) were negative, and no viral agent was detected in stool samples or throat swabs (limited panel). CRP concentration was high (189.6 g/liter). Empiric treatment with cefotaxim was administered for 6 d in hospital, followed by amoxicillin-clavulanic acid for 5 d. At the age of 21 mo, the patient was treated with amoxicillin-clavulanic acid for otitis media, periorbital cellulitis, and lymphadenitis. At the age of 33 mo, she had scarlet fever (clinical diagnosis), which was treated with oral cefadroxil for 10 d. 1 mo later, she was admitted for high fever, exanthema, and bilateral crackles, corresponding to bilateral bronchopneumonia on x ray. A viral swab revealed adenovirus infection, and a throat swab was positive for *Streptococcus pyogenes*. She was treated with i.v. amoxicillin for 6 d and was discharged on oral amoxicillin. At the age of 3 yr and 1 mo, the patient was again admitted for high fever with cough and dehydration. Chest x ray showed bilateral bronchopneumonia. CRP concentration was 280 mg/liter. The patient was admitted for 1 wk, receiving i.v. amoxicillin-clavulanic acid, and then oral treatment with the same drugs for 5 d. Throat swabs remained adenovirus positive. At the age of 3 yr and 5 mo, the patient received ambulatory treatment with 70 mg/kg amoxicillin for 1 wk for pneumonia (CRP 80 mg/liter). 1 mo later, she underwent a basic immunological assessment elsewhere, which showed normal antibody levels and normal immunophenotyping but weak responses to the unconjugated pneumococcal vaccine. At the age of 3 yr and 9 mo, the patient was again hospitalized, for respiratory distress and high fever, corresponding to yet another episode of bronchopneumonia, with an upper respiratory tract swab testing positive for IAV. At this point, the patient was referred to Leuven University Hospital for immunological assessment. The patient suffered another episode of radiologically proven pneumonia at the age of 46 mo, for which she was treated as an outpatient with amoxicillin/clavulanic acid for 12 d. CRP concentration reached 150 mg/liter.

Upon referral, the patient appeared to be a healthy young girl. Cystic fibrosis and primary ciliary dyskinesia had been excluded as underlying diagnoses. Immune screening was normal except for the borderline anti-pneumococcal response.

Laboratory tests showed normal counts of total lymphocytes ($3,600 \times 10^6/\text{liter}$), and lymphocyte profiling detected nothing aberrant. Immunoglobulin analyses showed normal IgM levels of 0.99 g/liter, IgG levels of 9.0 g/liter, and IgA levels of 0.73 g/liter. Trio WES was therefore performed, and the patient was placed on azithromycin prophylaxis while awaiting the results. Annual flu vaccination was recommended, and the patient received two shots of the COVID-19 BNT162b16 vaccine (Pfizer) off-label. Her vaccination schedule is otherwise up to date, and no adverse events were noted following vaccination with MMR. She is currently well and off all treatment. We have discussed the option of immunoglobulin prophylaxis with the parents, but, for now, close clinical observation is preferred.

Genetics

The methods used for high-throughput sequencing have been described elsewhere (Zhang et al., 2020). In brief, genomic DNA was extracted from whole blood. For WES, libraries were generated with the Twist Bioscience kit (Twist Human Core Exome Kit), the xGen Exome Research Panel from Integrated DNA Technologies (IDT xGen), the Agilent SureSelect V7 kit, or the SeqCap EZ MedExome kit (Roche). Massively parallel sequencing was performed on a NovaSeq6000 system (Illumina). We used the Genome Analysis Software Kit (v3.4-46 or 4; GATK) best-practice pipeline to analyze our WES data (DePristo et al., 2011). We aligned the reads obtained with the human reference genome (hg19), using the maximum exact matches algorithm in the Burrows-Wheeler Aligner (Li and Durbin, 2009). PCR duplicates were removed with Picard tools (<http://picard.sourceforge.net>). The GATK base quality score recalibrator was applied to correct sequencing artifacts. For P5 and P6, Illumina whole-genome sequencing, mapping, and read processing and annotation were performed according to the molecular inversion probe rare disease pipeline used at the Genomic Medicine Center Karolinska Rare Diseases (Stranneheim et al., 2021). Results were confirmed by Sanger sequencing.

All the variants were manually curated with Integrative Genomics Viewer and confirmed to affect the main functional protein isoform by verifying the protein sequence before inclusion in further analyses. The main functional protein isoform for IRF7 is NM_001572.5 (Zhang et al., 2020).

Cells

Blood samples were obtained in heparin-treated tubes from patients or from healthy human donor buffy coats or heparin-treated whole-blood samples (Karolinska University Hospital). PBMCs were isolated by density gradient centrifugation (Lymphoprep; STEMCELL Technologies) and resuspended in complete RPMI medium (RPMI 1640 with GlutaMAX [Gibco] supplemented with 10% FBS [Thermo Fisher Scientific]) for further analysis. HEK293T cells were cultured in DMEM supplemented with 10% FBS.

Evaluation of the stability and function of IRF7 variants in an ectopic expression system

HEK293T cells were cotransfected with a mixture of the IFN- β -firefly luciferase reporter plasmid, the pRL-TK-Renilla luciferase

plasmid, and the pcDNA3-IRF7 plasmid. Cells were incubated for 24 h and were then either left untreated or infected with Sendai virus (20 units/well) for another 24 h. Reporter activity was measured with the Dual-Luciferase Reporter Assay System, and all experiments were performed in technical triplicates. Firefly luciferase activity was normalized against *Renilla* luciferase activity. IRF7 levels were assessed by Western blotting using anti-IRF7 antibody (clone D2A1J; Cell Signaling) and anti-FLAG antibody (clone M2; Sigma-Aldrich). Membranes were reprobed for HRP-conjugated GAPDH (clone 1E6D9; PTG Lab) as a protein loading control.

Assessment of IRF7 levels in patients

Thawed PBMCs from cryopreserved samples (1×10^6 cells/well) were stimulated by incubation in complete RPMI in a 24-well plate. Cells were stimulated with 1,000 U/ml IFN- β (PBL Assay Science) or left unstimulated for 24 h at 37°C under an atmosphere containing 5% CO₂. At the end of the assay, the cells were harvested, washed in PBS, and the cell pellets were frozen at -20°C. Total cell lysates were subsequently prepared by lysis in radioimmunoprecipitation assay buffer (Thermo Fisher Scientific) with the inhibitors PMSF (ChemCruz) and sodium orthovanadate (ChemCruz), on ice for 1 h. The lysates were then denatured by heating at 70°C for 10 min in NuPAGE LDS sample buffer (Invitrogen) with 50 mM 1,4-dithiothreitol (Sigma-Aldrich) and resolved by gel electrophoresis in NuPAGE 4–12% Bis-Tris gels (Thermo Fisher Scientific). The protein bands were then transferred onto polyvinylidene difluoride membranes with the iBlot 2 Dry Blotting System (Thermo Fisher Scientific). Membranes were probed with anti-IRF7 antibody (#4920; Cell Signaling Technology) followed by HRP-conjugated anti-rabbit secondary antibody (Invitrogen). The membranes were then stripped and reprobed with HRP-anti-actin antibody (Invitrogen) as a protein loading control. Bands were visualized by enhanced chemiluminescence with the SuperSignal West Dura Extended Duration Substrate (Thermo Fisher Scientific) on an Odyssey Imaging System (LI-COR Biosciences).

Antibodies for flow cytometry

We used the following antibodies from BD Biosciences: BUV805-anti-human CD3 (clone UCHT1), BV711-anti-human CD11c (clone B-ly6), BUV395-anti-human CD56 (clone B159), PE-Cy7-anti-human CD95 (clone DX2), and PE-anti-human TNF (clone MAb11). The following antibodies were obtained from BioLegend: BV421-anti-human CCR7 (clone G043H7), BV711-anti-human CD8a (clone SK1), BV510-anti-human CD14 (clone M5E2), BV510-anti-human CD19 (clone HIB19), PE-Cy7-anti-human CD123 (clone 6H6), BV421-anti-human CD303 (BDCA-2; clone 201A), BV785-anti-human HLA-DR (clone L243), and FITC-anti-human IFN- γ (clone 4S.B3). The Qdot605-anti-human CD4 (clone S3.5) antibody was obtained from Thermo Fisher Scientific. The following antibodies were obtained from Miltenyi Biotec: FITC-anti-human CD141 (BDCA-3; clone AD5-14H12) and APC-anti-human IFN- α (clone LT27:295).

TLR stimulation of DCs

Freshly isolated PBMCs or thawed PBMCs from cryopreserved samples (1.5×10^6 cells/well) were stimulated in complete RPMI

in flat-bottom 96-well plates. For cryopreserved cells, stimulations were performed on freshly thawed cells, except for imiquimod stimulations, which were performed after allowing the cells to rest overnight. Cells were stimulated with 4 μ g/ml imiquimod (Alfa Aesar), 2 μ M CpG ODN 2336 (InvivoGen), 10 μ g/ml poly(I:C) (Miltenyi Biotec) or left unstimulated for 6 h in total at 37°C, under an atmosphere containing 5% CO₂. The addition of GolgiPlug (BD Biosciences) was optimized for each set of conditions. GolgiPlug was added after 1.5 h of stimulation for imiquimod, 3 h after stimulation for poly(I:C), or 4.5 h after stimulation for ODN.

At the end of the assay, cells were collected and incubated with CF430 viability dye (Biotium) and cell-surface antibody cocktails in FACS buffer (PBS supplemented with 1% FBS and 10 mM EDTA) at room temperature for 20 min. Cells were then fixed by incubation in 2% formaldehyde (Sigma-Aldrich) at room temperature for 15 min. The cells were permeabilized by washing twice in BD Perm/Wash Buffer (BD Biosciences) and stained for intracellular markers in Perm/Wash at room temperature for 30 min. Cells were then washed in Perm/Wash and finally resuspended in FACS buffer for acquisition on a BD FACSymphony flow cytometer (BD Biosciences) and analysis with FlowJo software (v10; BD Biosciences).

Peptide stimulation of T cells

Thawed PBMCs from cryopreserved samples (1×10^6 cells/well) were stimulated in U-bottom 96-well plates with 0.5 μ g/ml pooled peptides or 10 ng/ml PMA (Sigma-Aldrich) plus 0.5 μ M ionomycin (Sigma-Aldrich) in complete RPMI. The following peptide pools were used: CEFX Ultra SuperStim Pool MHC-I Subset (JPT Peptide Technologies), HCMV IE-1 (JPT Peptide Technologies), HCMV IE-2 (JPT Peptide Technologies), HCMV pp65 (JPT Peptide Technologies), EBV BLZF with 100 μ g/ml EBNA1 (Peptides & Elephants), Peptivator H1N1 HA (Miltenyi Biotec), Peptivator H1N1 MP1 (Miltenyi Biotec), Peptivator H1N1 MP2 (Miltenyi Biotec), Peptivator H1N1 NA (Miltenyi Biotec), Peptivator H1N1 NP (Miltenyi Biotec), Peptivator SARS-CoV-2 Prot-N (Miltenyi Biotec), and Peptivator SARS-CoV-2 Prot-S Complete (Miltenyi Biotec). Cells were stimulated for 6 h total at 37°C under an atmosphere containing 5% CO₂, with the addition of GolgiPlug (BD Biosciences) after 30 min of stimulation. At the end of the assay, cells were collected and incubated with CF430 viability dye (Biotium) and cell-surface antibody cocktail in FACS buffer (PBS supplemented with 1% FBS and 10 mM EDTA) at room temperature for 20 min. Cells were then fixed by incubation in 2% formaldehyde (Sigma-Aldrich) at room temperature for 15 min. The cells were permeabilized by washing twice in BD Perm/Wash Buffer (BD Biosciences), before staining for intracellular markers in Perm/Wash at room temperature for 30 min. The cells were then washed in Perm/Wash and resuspended in FACS buffer for acquisition on a BD FACSymphony flow cytometer (BD Biosciences) and analysis with FlowJo software (v10; BD Biosciences).

Whole-blood assays of T cell-specific antigen responses

Flow cytometry assays for specific cell-mediated immune responses in activated whole blood were performed as previously

described, to quantify CD4⁺ and CD8⁺ T cell blasts after 6 d of antigen stimulation (Lind Enoksson et al., 2021; Marits et al., 2014). Briefly, heparin-treated whole blood was diluted 1:10 in GlutaMAX RPMI 1640 (supplemented with 2 mM L-glutamine, 100 IU/ml penicillin, and 100 IU/ml streptomycin). In a U-bottom 96-well plate, cells were stimulated with influenza inactivated split-virus quadrivalent vaccine (Vaxigrip Tetra; Sanofi Pasteur) or UV-inactivated supernatant from cells infected with SARS-CoV-2 (The Public Health Agency of Sweden) at 37°C under an atmosphere containing 5% CO₂. After 6 d of incubation, the samples were stained with FITC-anti-human CD3 (clone SK7) and PE-anti-human CD4 (clone SK3) antibodies from BD Simultest (BD Biosciences), and erythrocytes were lysed in IOTest lysing solution (Beckman Coulter). Samples were acquired on a Cytoflex S flow cytometer (Beckman Coulter) and analyzed with KaluzaC software (Beckman Coulter). Blasts were identified as cells with high forward scatter, and the results are expressed as blasts/μl of whole blood.

VirScan

Patient serum samples were analyzed with VirScan as previously described (Xu et al., 2015). Briefly, an oligonucleotide library encoding 56-amino acid peptides tiling across the genomes of 206 viral species was synthesized on a releasable DNA microarray and cloned in the T7 phage. Patient serum samples containing 2 μg of IgG were added to the phage library, and immunoprecipitation was performed with Protein A and G beads. Peptides displaying enrichment in the samples were identified by PCR and Illumina sequencing of the peptide cassette from the immunoprecipitated phage.

RNA-seq

Previously published (Zhang et al., 2020; Sequence Read Archive accession no. PRJNA833449) RNA-seq data was reanalyzed to assess the differential expression of type I and type III IFN genes, as well as curated lists of ISGs (van der Wijst et al., 2021) and inflammatory genes (Liberzon et al., 2011), in isolated pDCs from P2 and a healthy control either unstimulated or cultured with SARS-CoV-2 or IAV.

Statistics

Statistical analyses were performed with Prism software (GraphPad).

Online supplemental material

Fig. S1 shows RNA-seq analysis of pDCs from P2 and a healthy control cultured with SARS-CoV-2 or IAV, focusing on IFN and inflammatory gene expression. Fig. S2 shows that BDCA-3⁺ DCs from patients P5, P6, and P7 produce levels of TNF similar to healthy controls following PBMC stimulation with TLR3 agonist poly(I:C). Fig. S3 shows patients that P5 and P6 had significantly stronger CD4⁺ T cell blast responses to influenza virus vaccine stimulation than healthy controls and similar T cell blast responses to SARS-CoV-2 compared to healthy convalescent controls. Fig. S3 also depicts VirScan analysis of all patients showing serological evidence of prior exposure to many common pathogens and responses to IAV and coronavirus antigens. Table

S1 details the nine biallelic patient-associated *IRF7* variants, all nonsynonymous or splicing site variants of *IRF7* present in a homozygous state in at least one individual reported in the public gnomAD database, and all *IRF7* variants present in a heterozygous state in the gnomAD database with a MAF >0.0001.

Acknowledgments

We thank the patients and their families for participating in our research. Sequencing was performed at the SciLifeLab Clinical Genomics Facility. We thank the MedH Flow Cytometry Core Facility of the Karolinska Institute for providing cell analysis services. The graphical abstract was created with BioRender.

This work was supported by the Swedish Research Council, Göran Gustafsson Foundation, Karolinska Institute Doctoral Program, Center for Innovative Medicine (CIMED; to Y.T. Bryceson), CIMED (to C.I.E. Smith), and CIMED, Stockholm County Council and Karolinska Institute (to P. Bergman). Part of this work was generated within the European Reference Network for rare primary immunodeficiency, autoinflammatory and autoimmune diseases (to C.I.E. Smith and P. Bergman). T.M. Campbell is supported by a Swedish Society for Medical Research postdoctoral grant. The Laboratory of Human Genetics of Infectious Diseases is supported by the Howard Hughes Medical Institute, the Rockefeller University, the St. Giles Foundation, the National Institutes of Health (NIH; R01AI088364 and R01AI63029), the National Center for Advancing Translational Sciences, NIH Clinical and Translational Science Award program (UL1 TR001866), a Fast Grant from Emergent Ventures, the Mercatus Center at George Mason University, the Yale Center for Mendelian Genomics and the GSP Coordinating Center funded by the National Human Genome Research Institute (UM1HG006504 and U24HG008956), the Yale High-Performance Computing Center (S100D018521), the Fisher Center for Alzheimer's Research Foundation, the JPB Foundation, the Meyer Foundation, the French National Research Agency (ANR) under the "Investments for the Future" program (ANR-10-IAHU-01), the Integrative Biology of Emerging Infectious Diseases Laboratory of Excellence (ANR-10-LABX-62-IBEID), the French Foundation for Medical Research (FRM; EQU201903007798), the ANR GenMISC (ANR-21-COVR-039), the ANRS-COV05, ANR GENVIR (ANR-20-CE93-003) and ANR AABIFNCOV (ANR-20-CO11-0001) projects, the European Union's Horizon 2020 Research and Innovation Program under grant agreement no. 824110 (EASI-genomics), the Square Foundation, Grandir - Fonds de solidarité pour l'enfance, Fondation du Souffle, the SCOR Corporate Foundation for Science, The French Ministry of Higher Education, Research, and Innovation (MESRI-COVID-19), Institut National de la Santé et de la Recherche Médicale (INSERM), REACTing-INSERM, and the University of Paris. P. Bastard was supported by the MD-PhD program of the Imagine Institute (with the support of the Bettencourt-Schueller Foundation). I. Meyts is a senior clinical investigator at the Research Foundation - Flanders and is supported by the CSL Behring Chair of Primary Immunodeficiencies, a KU Leuven C1 Grant (grant number C16/18/007), a VIB GC PID Grant, the Research Foundation - Flanders (grant numbers G0C8517N, G0B5120N and

GOE8420N), and the Jeffrey Modell Foundation. I. Migeotte is funded by Fonds Erasme. This work was supported by ERN-RITA.

Author contributions: Conceptualization, Q. Zhang, I. Meyts, J.-L. Casanova, and Y.T. Bryceson; Methodology, T.M. Campbell, Z. Liu, M. Moncada-Velez, L.E. Covill, P. Bastard, L. Bizien, S. Lind Enoksson, T. Khan, Y. Kendir-Demirkol, A.A. Arias, P. Marits, and N. Marr; Patient care and clinical data analysis, Q. Zhang, I. Alavi Darazam, P. Bastard, G. Bucciol, E. Jouanguy, S.N. Karabela, I. Migeotte, D. Mansouri, L. Moens, T. Ozelik, I. Pellier, A. Sendel, S. Şenoğlu, M. Shahrooei, C.I.E. Smith, I. Vandernoot, K. Willekens, K. Kart Yaşar, P. Bergman, L. Abel, A. Cobat, and C.H.G.E. authors; Writing—original draft, T.M. Campbell, Q. Zhang, I. Meyts, J.-L. Casanova, and Y.T. Bryceson; Writing—review & editing, all authors; Funding acquisition, T.M. Campbell, Q. Zhang, I. Meyts, L. Abel, J.-L. Casanova, and Y.T. Bryceson; Supervision, I. Meyts, J.-L. Casanova, and Y.T. Bryceson.

Disclosures: J.-L. Casanova reported a patent to PCT/US2021/042741 pending. I. Meyts reported grants from CSL Behring—paid to KU Leuven outside the submitted work. No other disclosures were reported.

Submitted: 3 February 2022

Revised: 29 March 2022

Accepted: 12 May 2022

References

- Abolhassani, H., N. Landegren, P. Bastard, M. Materna, M. Modaresi, L. Du, M. Aranda-Guillen, F. Sardh, F. Zuo, P. Zhang, et al. 2022. Inherited IFNAR1 deficiency in a child with both critical COVID-19 pneumonia and multisystem inflammatory syndrome. *J. Clin. Immunol.* 42:471–483. <https://doi.org/10.1007/s10875-022-01215-7>
- Alosaimi, M.F., M.C. Maciag, C.D. Platt, R.S. Geha, J. Chou, and L.M. Bartnikas. 2019. A novel variant in STAT2 presenting with hemophagocytic lymphohistiocytosis. *J. Allergy Clin. Immunol.* 144:611–613.e3. <https://doi.org/10.1016/j.jaci.2019.05.008>
- Asano, T., B. Boisson, F. Onodi, D. Matuozzo, M. Moncada-Velez, M.R.L. Maglorius Renkilaraj, P. Zhang, L. Meertens, A. Bolze, M. Materna, et al. 2021. X-linked recessive TLR7 deficiency in ~1% of men under 60 years old with life-threatening COVID-19. *Sci. Immunology*. 6:eabl4348. <https://doi.org/10.1126/sciimmunol.abl4348>
- Bastard, P., K.C. Hsiao, Q. Zhang, J. Choin, E. Best, J. Chen, A. Gervais, L. Bizien, M. Materna, C. Harmant, et al. 2022. A loss-of-function IFNAR1 allele in Polynesia underlies severe viral diseases in homozygotes. *J. Exp. Med.* 219:e20220028. <https://doi.org/10.1084/jem.20220028>
- Bastard, P., J. Manry, J. Chen, J. Rosain, Y. Seeleuthner, O. AbuZaitun, L. Lorenzo, T. Khan, M. Hasek, N. Hernandez, et al. 2021. Herpes simplex encephalitis in a patient with a distinctive form of inherited IFNAR1 deficiency. *J. Clin. Invest.* 131:e139980. <https://doi.org/10.1172/jci139980>
- Bidwell, B.N., C.Y. Slaney, N.P. Withana, S. Forster, Y. Cao, S. Loi, D. Andrews, T. Mikeska, N.E. Mangan, S.A. Samarajiwa, et al. 2012. Silencing of Irf7 pathways in breast cancer cells promotes bone metastasis through immune escape. *Nat. Med.* 18:1224–1231. <https://doi.org/10.1038/nm.2830>
- Blanco-Melo, D., B.E. Nilsson-Payant, W.C. Liu, S. Uhl, D. Hoagland, R. Moller, T.X. Jordan, K. Oishi, M. Panis, D. Sachs, et al. 2020. Imbalanced host response to SARS-CoV-2 drives development of COVID-19. *Cell*. 181:1036–1045.e9. <https://doi.org/10.1016/j.cell.2020.04.026>
- Boehmer, D.F.R., L.M. Koehler, T. Magg, M. Metzger, M. Rohlf, J. Ahlfeld, A. Rack-Hoch, K. Reiter, M.H. Albert, S. Endres, et al. 2020. A novel complete autosomal-recessive STAT1 LOF variant causes immunodeficiency with hemophagocytic lymphohistiocytosis-like hyperinflammation. *J. Allergy Clin. Immunol. Pract.* 8:3102–3111. <https://doi.org/10.1016/j.jaip.2020.06.034>
- Bradley, P., and P.G. Thomas. 2019. Using T cell receptor repertoires to understand the principles of adaptive immune recognition. *Annu. Rev. Immunol.* 37:547–570. <https://doi.org/10.1146/annurev-immunol-042718-041757>
- Burns, C., A. Cheung, Z. Stark, S. Choo, L. Downie, S. White, R. Conyers, and T. Cole. 2016. A novel presentation of homozygous loss-of-function STAT-1 mutation in an infant with hyperinflammation—A case report and review of the literature. *J. Allergy Clin. Immunol. Pract.* 4:777–779. <https://doi.org/10.1016/j.jaip.2016.02.015>
- Casanova, J.L., and L. Abel. 2021. Mechanisms of viral inflammation and disease in humans. *Science*. 374:1080–1086. <https://doi.org/10.1126/science.abj7965>
- Casanova, J.L., H.C. Su, and C.H.G. Effort. 2020. A global effort to define the human genetics of protective immunity to SARS-CoV-2 infection. *Cell*. 181:1194–1199. <https://doi.org/10.1016/j.cell.2020.05.016>
- Cella, M., D. Jarrossay, F. Facchetti, O. Alebardi, H. Nakajima, A. Lanzavecchia, and M. Colonna. 1999. Plasmacytoid monocytes migrate to inflamed lymph nodes and produce large amounts of type I interferon. *Nat. Med.* 5:919–923. <https://doi.org/10.1038/11360>
- Chapigier, A., R.F. Wynn, E. Jouanguy, O. Filipe-Santos, S. Zhang, J. Feinberg, K. Hawkins, J.L. Casanova, and P.D. Arkwright. 2006. Human complete Stat-1 deficiency is associated with defective type I and II IFN responses in vitro but immunity to some low virulence viruses in vivo. *J. Immunol.* 176:5078–5083. <https://doi.org/10.4049/jimmunol.176.8.5078>
- Chu, H., J.F.-W. Chan, Y. Wang, T.T.-T. Yuen, Y. Chai, Y. Hou, H. Shuai, D. Yang, B. Hu, X. Huang, et al. 2020. Comparative replication and immune activation profiles of SARS-CoV-2 and SARS-CoV in human lungs: An ex vivo study with implications for the pathogenesis of COVID-19. *Clin. Infect. Dis.* 71:1400–1409. <https://doi.org/10.1093/cid/ciaa410>
- Ciancanelli, M.J., L. Abel, S.Y. Zhang, and J.L. Casanova. 2016. Host genetics of severe influenza: From mouse Mx1 to human IRF7. *Curr. Opin. Immunol.* 38:109–120. <https://doi.org/10.1016/j.coi.2015.12.002>
- Ciancanelli, M.J., S.X.L. Huang, P. Luthra, H. Garner, Y. Itan, S. Volpi, F.G. Lafaille, C. Trouillet, M. Schmolke, R.A. Albrecht, et al. 2015. Infectious disease. Life-threatening influenza and impaired interferon amplification in human IRF7 deficiency. *Science*. 348:448–453. <https://doi.org/10.1126/science.aaa1578>
- Colonna, M., G. Trinchieri, and Y.J. Liu. 2004. Plasmacytoid dendritic cells in immunity. *Nat. Immunol.* 5:1219–1226. <https://doi.org/10.1038/ni1141>
- Crouse, J., G. Bedenikovic, M. Wiesel, M. Ibberson, I. Xenarios, D. Von Laer, U. Kalinke, E. Vivier, S. Jonjic, and A. Oxenius. 2014. Type I interferons protect T cells against NK cell attack mediated by the activating receptor NCR1. *Immunity*. 40:961–973. <https://doi.org/10.1016/j.immuni.2014.05.003>
- Crouse, J., U. Kalinke, and A. Oxenius. 2015. Regulation of antiviral T cell responses by type I interferons. *Nat. Rev. Immunol.* 15:231–242. <https://doi.org/10.1038/nri3806>
- Duncan, C.J.A., M.K. Skouboe, S. Howarth, A.K. Hollensen, R. Chen, M.L. Borresen, B.J. Thompson, J. Stremenova Spegarova, C.F. Hatton, F.F. Staeger, et al. 2022. Life-threatening viral disease in a novel form of autosomal recessive IFNAR2 deficiency in the Arctic. *J. Exp. Med.* 219:e20212427. <https://doi.org/10.1084/jem.20212427>
- Duncan, C.J.A., S.M.B. Mohamad, D.F. Young, A.J. Skelton, T.R. Leahy, D.C. Munday, K.M. Butler, S. Morfopoulou, J.R. Brown, M. Hubank, et al. 2015. Human IFNAR2 deficiency: Lessons for antiviral immunity. *Sci. Transl. Med.* 7:307ra154. <https://doi.org/10.1126/scitranslmed.aac4227>
- DePristo, M.A., E. Banks, R. Poplin, K.V. Garimella, J.R. Maguire, C. Hartl, A.A. Philippakis, G. del Angel, M.A. Rivas, and M. Hanna. 2011. A framework for variation discovery and genotyping using next-generation DNA sequencing data. *Nat. Genet.* 43:491–498. <https://doi.org/10.1038/ng.806>
- Duncan, C.J.A., R.E. Randall, and S. Hambleton. 2021. Genetic lesions of type I interferon signalling in human antiviral immunity. *Trends Genet.* 37:46–58. <https://doi.org/10.1016/j.tig.2020.08.017>
- Dupuis, S., E. Jouanguy, S. Al-Hajjar, C. Fieschi, I.Z. Al-Mohsen, S. Al-Jumaah, K. Yang, A. Chapigier, C. Eidenschenk, P. Eid, et al. 2003. Impaired response to interferon-alpha/beta and lethal viral disease in human STAT1 deficiency. *Nat. Genet.* 33:388–391. <https://doi.org/10.1038/ng1097>
- Fung, K.Y., N.E. Mangan, H. Cumming, J.C. Horvat, J.R. Mayall, S.A. Stifter, N. De Weerd, L.C. Roisman, J. Rossjohn, S.A. Robertson, et al. 2013. Interferon-epsilon protects the female reproductive tract from viral and bacterial infection. *Science*. 339:1088–1092. <https://doi.org/10.1126/science.1233321>

- Gao, D., M.J. Ciancanelli, P. Zhang, O. Harschnitz, V. Bondet, M. Hasek, J. Chen, X. Mu, Y. Itan, A. Cobat, et al. 2021. TLR3 controls constitutive IFN-beta antiviral immunity in human fibroblasts and cortical neurons. *J. Clin. Invest.* 131:e134529. <https://doi.org/10.1172/JCI134529>
- Garcia-Sastre, A. 2017. Ten strategies of interferon evasion by viruses. *Cell Host Microbe*. 22:176–184. <https://doi.org/10.1016/j.chom.2017.07.012>
- Gothe, F., C.F. Hatton, L. Truong, Z. Klimova, V. Kanderova, M. Fejtkova, A. Grainger, V. Bigley, J. Perthen, D. Mitra, et al. 2020. A novel case of homozygous (IFNAR1) deficiency with haemophagocytic lymphohistiocytosis. *Clin. Infect. Dis.* 74:136–139. <https://doi.org/10.1093/cid/ciaa1790>
- Hambleton, S., S. Goodbourn, D.F. Young, P. Dickinson, S.M.B. Mohamad, M. Valappil, N. McGovern, A.J. Cant, S.J. Hackett, P. Ghazal, et al. 2013. STAT2 deficiency and susceptibility to viral illness in humans. *Proc. Natl. Acad. Sci. USA*. 110:3053–3058. <https://doi.org/10.1073/pnas.1220098110>
- Harris, B.D., J. Schreiter, M. Chevrier, J.L. Jordan, and M.R. Walter. 2018. Human interferon- and interferon-kappa exhibit low potency and low affinity for cell-surface IFNAR and the poxvirus antagonist B18R. *J. Biol. Chem.* 293:16057–16068. <https://doi.org/10.1074/jbc.RA118.003617>
- Hatesuer, B., H.T.T. Hoang, P. Riese, S. Trittel, I. Gerhauser, H. Elbahesh, R. Geffers, E. Wilk, and K. Schughart. 2017. Deletion of Irf3 and Irf7 genes in mice results in altered interferon pathway activation and granulocyte-dominated inflammatory responses to influenza A infection. *J. Innate Immun.* 9:145–161. <https://doi.org/10.1159/000450705>
- Hernandez, N., G. Bucciol, L. Moens, J. Le Pen, M. Shahrooei, E. Goudouris, A. Shirvani, M. Changi-Ashtiani, H. Rokni-Zadeh, E.H. Sayar, et al. 2019. Inherited IFNAR1 deficiency in otherwise healthy patients with adverse reaction to measles and yellow fever live vaccines. *J. Exp. Med.* 216:2057–2070. <https://doi.org/10.1084/jem.20182295>
- Hernandez, N., I. Melki, H. Jing, T. Habib, S.S.Y. Huang, J. Danielson, T. Kula, S. Drutman, S. Belkaya, V. Rattina, et al. 2018. Life-threatening influenza pneumonitis in a child with inherited IRF9 deficiency. *J. Exp. Med.* 215:2567–2585. <https://doi.org/10.1084/jem.20180628>
- Hoffmann, H.H., W.M. Schneider, and C.M. Rice. 2015. Interferons and viruses: An evolutionary arms race of molecular interactions. *Trends Immunol.* 36:124–138. <https://doi.org/10.1016/j.it.2015.01.004>
- Honda, K., and T. Taniguchi. 2006. IRFs: Master regulators of signalling by Toll-like receptors and cytosolic pattern-recognition receptors. *Nat. Rev. Immunol.* 6:644–658. <https://doi.org/10.1038/nri1900>
- Honda, K., H. Yanai, H. Negishi, M. Asagiri, M. Sato, T. Mizutani, N. Shimada, Y. Ohba, A. Takaoka, N. Yoshida, and T. Taniguchi. 2005. IRF-7 is the master regulator of type-I interferon-dependent immune responses. *Nature*. 434:772–777. <https://doi.org/10.1038/nature03464>
- Hong, X.X., and G.G. Carmichael. 2013. Innate immunity in pluripotent human cells: Attenuated response to interferon- β . *J. Biol. Chem.* 288:16196–16205. <https://doi.org/10.1074/jbc.M112.435461>
- Itan, Y., L. Shang, B. Boisson, M.J. Ciancanelli, J.G. Markle, R. Martinez-Barricarte, E. Scott, I. Shah, P.D. Stenson, J. Gleeson, et al. 2016. The mutation significance cutoff: Gene-level thresholds for variant predictions. *Nat. Methods*. 13:109–110. <https://doi.org/10.1038/nmeth.3739>
- Jongbloed, S.L., A.J. Kassianos, K.J. McDonald, G.J. Clark, X. Ju, C.E. Angel, C.J.J. Chen, P.R. Dunbar, R.B. Wadley, V. Jeet, et al. 2010. Human CD141+ (BDCA-3)+ dendritic cells (DCs) represent a unique myeloid DC subset that cross-presents necrotic cell antigens. *J. Exp. Med.* 207:1247–1260. <https://doi.org/10.1084/jem.20092140>
- Karczewski, K.J., L.C. Francioli, G. Tiao, B.B. Cummings, J. Alfoldi, Q. Wang, R.L. Collins, K.M. Laricchia, A. Ganna, D.P. Birnbaum, et al. 2020. The mutational constraint spectrum quantified from variation in 141,456 humans. *Nature*. 581:434–443. <https://doi.org/10.1038/s41586-020-2308-7>
- Kircher, M., D.M. Witten, P. Jain, B.J. O’Roak, G.M. Cooper, and J. Shendure. 2014. A general framework for estimating the relative pathogenicity of human genetic variants. *Nat. Genet.* 46:310–315. <https://doi.org/10.1038/ng.2892>
- LaFleur, D.W., B. Nardelli, T. Tsareva, D. Mather, P. Feng, M. Semenuk, K. Taylor, M. Buerger, D. Chinchilla, V. Roshke, et al. 2001. Interferon-kappa, a novel type I interferon expressed in human keratinocytes. *J. Biol. Chem.* 276:39765–39771. <https://doi.org/10.1074/jbc.M102502200>
- Lazear, H.M., J.W. Schoggins, and M.S. Diamond. 2019. Shared and distinct functions of type I and type III interferons. *Immunity*. 50:907–923. <https://doi.org/10.1016/j.immuni.2019.03.025>
- Le Voyer, T., S. Sakata, M. Tsumura, T. Khan, A. Esteve-Sole, B.K. Al-Saud, H.E. Gungor, P. Taur, V. Jeanne-Julien, M. Christiansen, et al. 2021. Genetic, immunological, and clinical features of 32 patients with autosomal recessive STAT1 deficiency. *J. Immunol.* 207:133–152. <https://doi.org/10.4049/jimmunol.2001451>
- Li, H., and R. Durbin. 2009. Fast and accurate short read alignment with Burrows-Wheeler transform. *Bioinformatics*. 25:1754–1760. <https://doi.org/10.1093/bioinformatics/btp324>
- Liberzon, A., A. Subramanian, R. Pinchback, H. Thorvaldsdottir, P. Tamayo, and J.P. Mesirov. 2011. Molecular signatures database (MSigDB) 3.0. *Bioinformatics*. 27:1739–1740. <https://doi.org/10.1093/bioinformatics/btr260>
- Lim, H.K., S.X.L. Huang, J. Chen, G. Kerner, O. Gilliaux, P. Bastard, K. Dobbs, N. Hernandez, N. Goudin, M.L. Hasek, et al. 2019. Severe influenza pneumonitis in children with inherited TLR3 deficiency. *J. Exp. Med.* 216:2038–2056. <https://doi.org/10.1084/jem.20181621>
- Lind Enoksson, S., P. Bergman, J. Klingstrom, F. Bostrom, R. Da Silva Rodrigues, M.E. Winerdal, and P. Marits. 2021. A flow cytometry-based proliferation assay for clinical evaluation of T-cell memory against SARS-CoV-2. *J. Immunol. Methods*. 499:113159. <https://doi.org/10.1016/j.jim.2021.113159>
- Liu, Y.J. 2001. Dendritic cell subsets and lineages, and their functions in innate and adaptive immunity. *Cell*. 106:259–262. [https://doi.org/10.1016/S0092-8674\(01\)00456-1](https://doi.org/10.1016/S0092-8674(01)00456-1)
- Marits, P., A.C. Wikstrom, D. Popadic, O. Winqvist, and S. Thunberg. 2014. Evaluation of T and B lymphocyte function in clinical practice using a flow cytometry based proliferation assay. *Clin. Immunol.* 153:332–342. <https://doi.org/10.1016/j.clim.2014.05.010>
- Meyts, I., and J.L. Casanova. 2021. Viral infections in humans and mice with genetic deficiencies of the type I IFN response pathway. *Eur. J. Immunol.* 51:1039–1061. <https://doi.org/10.1002/eji.202048793>
- Miyamoto, M., T. Fujita, Y. Kimura, M. Maruyama, H. Harada, Y. Sudo, T. Miyata, and T. Taniguchi. 1988. Regulated expression of a gene encoding a nuclear factor, IRF-1, that specifically binds to IFN-beta gene regulatory elements. *Cell*. 54:903–913. [https://doi.org/10.1016/S0092-8674\(88\)91307-4](https://doi.org/10.1016/S0092-8674(88)91307-4)
- Moens, L., L. Van Eyck, D. Jochmans, T. Mitera, G. Frans, X. Bossuyt, P. Matthys, J. Neyts, M. Ciancanelli, S.Y. Zhang, et al. 2017. A novel kindred with inherited STAT2 deficiency and severe viral illness. *J. Allergy Clin. Immunol.* 139:1995–1997.e9. <https://doi.org/10.1016/j.jaci.2016.10.033>
- Poyhonen, L., J. Bustamante, J.L. Casanova, E. Jouanguy, and Q. Zhang. 2019. Life-threatening infections due to live-attenuated vaccines: Early manifestations of inborn errors of immunity. *J. Clin. Immunol.* 39:376–390. <https://doi.org/10.1007/s10875-019-00642-3>
- Rapaport, F., B. Boisson, A. Gregor, V. Beziat, S. Boisson-Dupuis, J. Bustamante, E. Jouanguy, A. Puel, J. Rosain, Q. Zhang, et al. 2021. Negative selection on human genes underlying inborn errors depends on disease outcome and both the mode and mechanism of inheritance. *Proc. Natl. Acad. Sci. USA*. 118:e2001248118. <https://doi.org/10.1073/pnas.2001248118>
- Reizis, B. 2019. Plasmacytoid dendritic cells: Development, regulation, and function. *Immunity*. 50:37–50. <https://doi.org/10.1016/j.immuni.2018.12.027>
- Sakata, S., M. Tsumura, T. Matsubayashi, S. Karakawa, S. Kimura, M. Tamaura, T. Okano, T. Naruto, Y. Mizoguchi, R. Kagawa, et al. 2020. Autosomal recessive complete STAT1 deficiency caused by compound heterozygous intronic mutations. *Int. Immunol.* 32:663–671. <https://doi.org/10.1093/intimm/dxaa043>
- Schneider, W.M., M.D. Chevillotte, and C.M. Rice. 2014. Interferon-stimulated genes: A complex web of host defenses. *Annu. Rev. Immunol.* 32:513–545. <https://doi.org/10.1146/annurev-immunol-032713-120231>
- Schoggins, J.W. 2019. Interferon-stimulated genes: What do they all do? *Annu. Rev. Virol.* 6:567–584. <https://doi.org/10.1146/annurev-virology-092818-015756>
- Shingai, M., T. Ebihara, N.A. Begum, A. Kato, T. Honma, K. Matsumoto, H. Saito, H. Ogura, M. Matsumoto, and T. Seya. 2007. Differential type I IFN-inducing abilities of wild-type versus vaccine strains of measles virus. *J. Immunol.* 179:6123–6133. <https://doi.org/10.4049/jimmunol.179.9.6123>
- Siegal, F.P., N. Kadowaki, M. Shodell, P.A. Fitzgerald-Bocarsly, K. Shah, S. Ho, S. Antonenko, and Y.J. Liu. 1999. The nature of the principal type 1 interferon-producing cells in human blood. *Science*. 284:1835–1837. <https://doi.org/10.1126/science.284.5421.1835>
- Sontag, S., M. Forster, J. Qin, P. Wanek, S. Mitzka, H.M. Schuler, S. Koschmieder, S. Rose-John, K. Sere, and M. Zenke. 2017. Modelling IRF8 deficient human hematopoiesis and dendritic cell development with engineered iPS cells. *Stem Cell*. 35:898–908. <https://doi.org/10.1002/stem.2565>

- Stranneheim, H., K. Lagerstedt-Robinson, M. Magnusson, M. Kvarnung, D. Nilsson, N. Lesko, M. Engvall, B.M. Anderlid, H. Arnell, C.B. Johansson, et al. 2021. Integration of whole genome sequencing into a healthcare setting: High diagnostic rates across multiple clinical entities in 3219 rare disease patients. *Genome Med.* 13:40. <https://doi.org/10.1186/s13073-021-00855-5>
- Vairo, D., L. Tassone, G. Tabellini, N. Tamassia, S. Gasperini, F. Bazzoni, A. Plebani, F. Porta, L.D. Notarangelo, S. Parolini, et al. 2011. Severe impairment of IFN-gamma and IFN-alpha responses in cells of a patient with a novel STAT1 splicing mutation. *Blood.* 118:1806–1817. <https://doi.org/10.1182/blood-2011-01-330571>
- van der Wijst, M.G.P., S.E. Vazquez, G.C. Hartoularos, P. Bastard, T. Grant, R. Bueno, D.S. Lee, J.R. Greenland, Y. Sun, R. Perez, et al. 2021. Type I interferon autoantibodies are associated with systemic immune alterations in patients with COVID-19. *Sci. Transl. Med.* 13:eabh2624. <https://doi.org/10.1126/scitranslmed.abh2624>
- Weekes, M.P., P. Tomasec, E.L. Huttlin, C.A. Fielding, D. Nusinow, R.J. Stanton, E.C.Y. Wang, R. Aicheler, I. Murrell, G.W.G. Wilkinson, et al. 2014. Quantitative temporal viromics: An approach to investigate host-pathogen interaction. *Cell.* 157:1460–1472. <https://doi.org/10.1016/j.cell.2014.04.028>
- Wu, X., V.L. Dao Thi, Y. Huang, E. Billerbeck, D. Saha, H.H. Hoffmann, Y. Wang, L.A.V. Silva, S. Sarbanes, T. Sun, et al. 2018. Intrinsic immunity shapes viral resistance of stem cells. *Cell.* 172:423–438.e25. <https://doi.org/10.1016/j.cell.2017.11.018>
- Xu, G.J., T. Kula, Q. Xu, M.Z. Li, S.D. Vernon, T. Ndung'u, K. Ruxrungtham, J. Sanchez, C. Brander, R.T. Chung, et al. 2015. Viral immunology. Comprehensive serological profiling of human populations using a synthetic human virome. *Science.* 348:aaa0698. <https://doi.org/10.1126/science.aaa0698>
- Zhang, P., B. Bigio, F. Rapaport, S.Y. Zhang, J.L. Casanova, L. Abel, B. Boisson, and Y. Itan. 2018. PopViz: A webserver for visualizing minor allele frequencies and damage prediction scores of human genetic variations. *Bioinformatics.* 34:4307–4309. <https://doi.org/10.1093/bioinformatics/bty536>
- Zhang, Q., P. Bastard, C.H.G. Effort, A. Cobat, and J.L. Casanova. 2022. Human genetic and immunological determinants of critical COVID-19 pneumonia. *Nature.* 603:587–598. <https://doi.org/10.1038/s41586-022-04447-0>
- Zhang, Q., P. Bastard, Z. Liu, J. Le Pen, M. Moncada-Velez, J. Chen, M. Ogishi, I.K.D. Sabli, S. Hodeib, C. Korol, et al. 2020. Inborn errors of type I IFN immunity in patients with life-threatening COVID-19. *Science.* 370:eabd4570. <https://doi.org/10.1126/science.abd4570>
- Zhang, S.Y., E. Jouanguy, S. Ugolini, A. Smahi, G. Elain, P. Romero, D. Segal, V. Sancho-Shimizu, L. Lorenzo, A. Puel, et al. 2007. TLR3 deficiency in patients with herpes simplex encephalitis. *Science.* 317:1522–1527. <https://doi.org/10.1126/science.1139522>
- Zhao, Y., W. Chen, W. Zhu, H. Meng, J. Chen, and J. Zhang. 2017. Overexpression of interferon regulatory factor 7 (IRF7) reduces bone metastasis of prostate cancer cells in mice. *Oncol. Res.* 25:511–522. <https://doi.org/10.3727/096504016X14756226781802>

Supplemental material

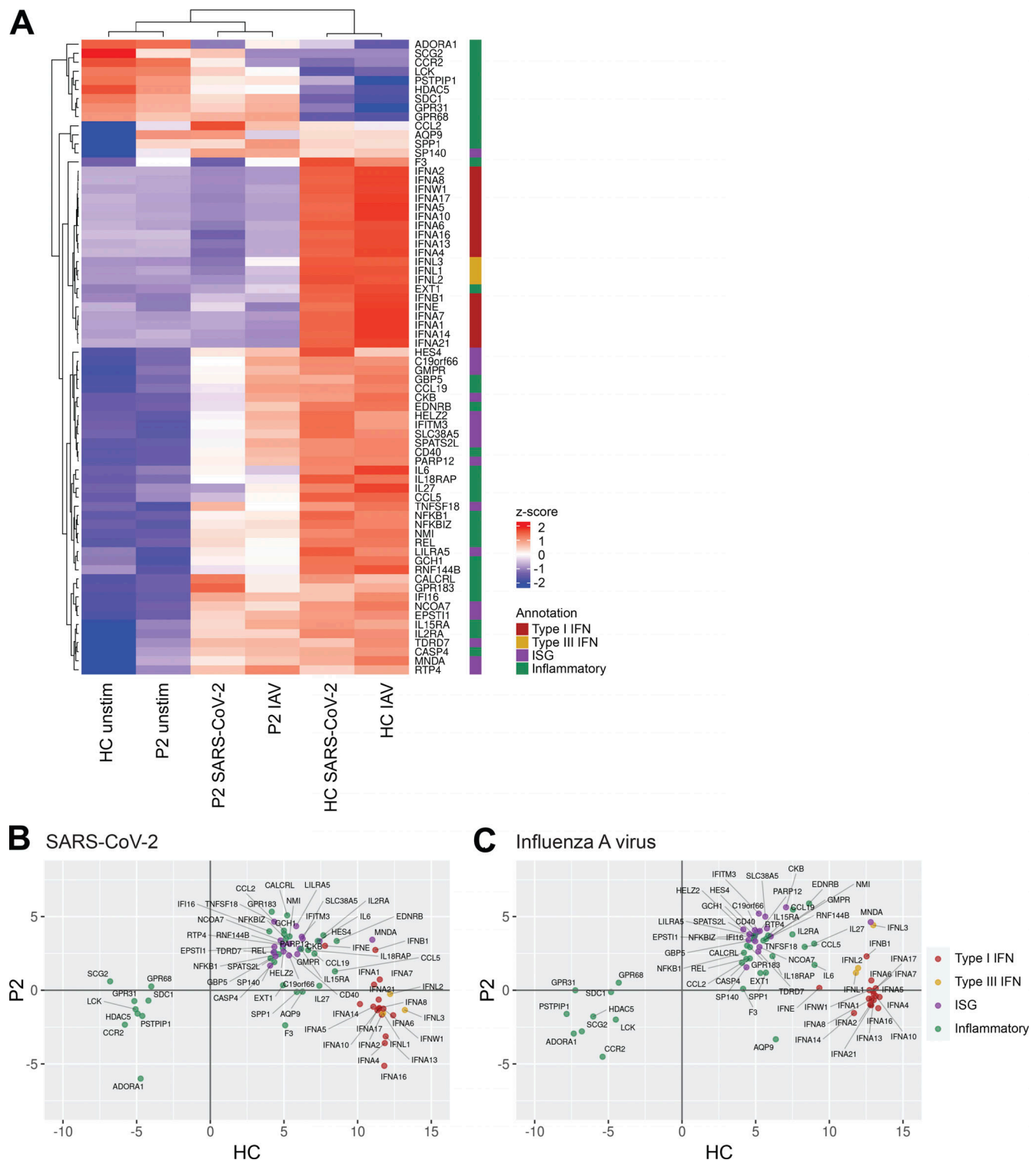


Figure S1. **IFN and inflammatory responses in IRF7-deficient pDCs challenged with SARS-CoV-2 and IAV.** RNA-seq analysis of isolated pDCs from P2 and a healthy control (HC) either unstimulated or cultured with SARS-CoV-2 or IAV. **(A–C)** Genes in the annotated interest groups with expression >2.5-fold higher or lower in P2 vs. HC after viral culture were plotted as a heatmap of expression z-score (A) and expression fold-change in P2 vs. HC (B and C). Data are representative of a single experiment and reanalyzed from [Zhang et al. \(2020\)](#).

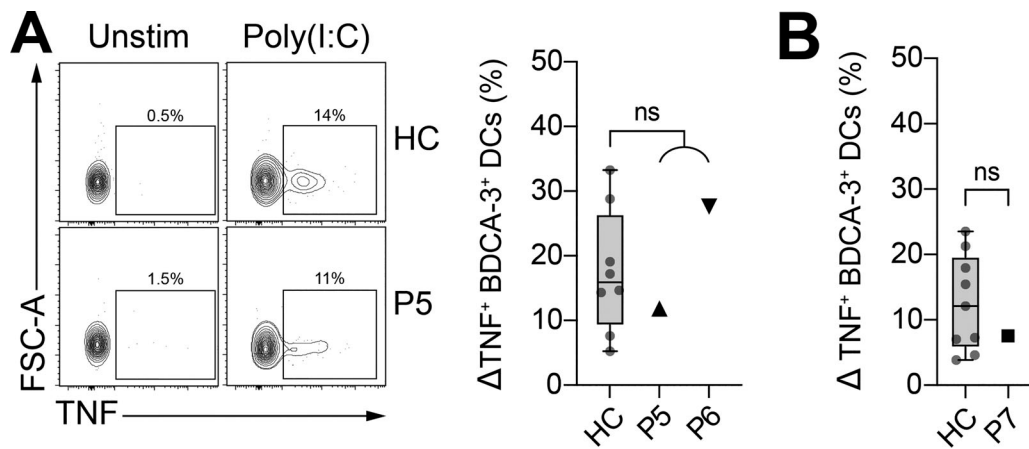


Figure S2. **Patients with newly discovered deleterious *IRF7* variants produce normal levels of TNF after the TLR3-mediated stimulation of BDCA3⁺ DCs.** (A and B) Frequency of TNF-producing BDCA3⁺ DCs (live Lin⁻CD123⁻HLA-DR⁺CD141⁺) after 6 h of stimulation with poly(I:C), for fresh (A) and thawed (B) PBMCs. All data are presented as the frequency of responding cells minus that of the respective unstimulated controls. Box plots are bound by the 25th and 75th percentiles. The median is marked, and the whiskers indicate the maximum and minimum. Individual values are plotted. Unpaired *t* tests were performed to compare healthy controls (HC; *n* = 8–9) and patients. FSC, forward scatter.

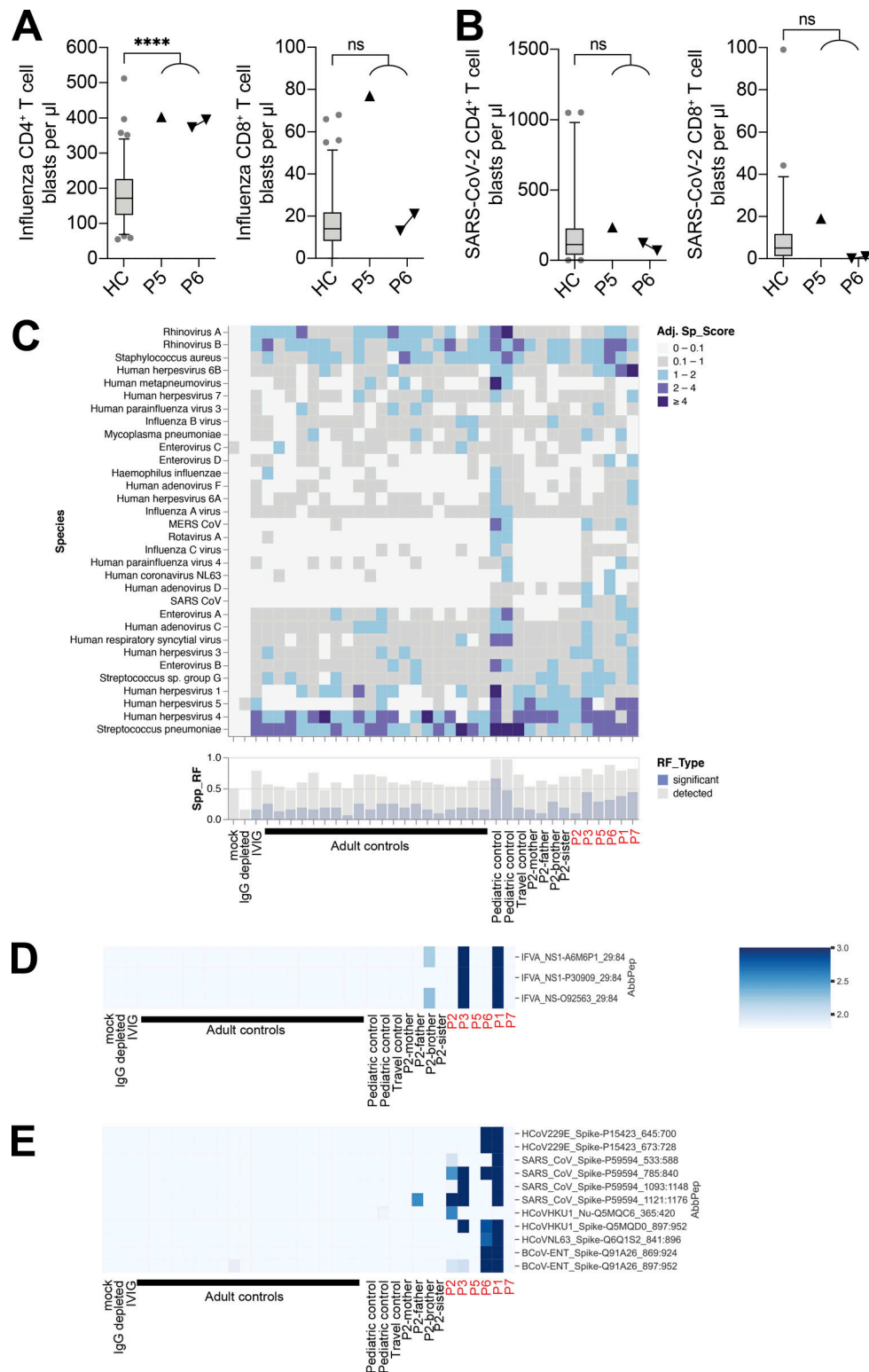


Figure S3. **Large numbers of influenza-specific CD4⁺ T cell blasts in IRF7-deficient patients.** (A and B) Whole-blood CD4⁺ (CD3⁺CD4⁺) and CD8⁺ (CD3⁺CD4⁻) T cell blast responses to influenza split-virus vaccine (A) or SARS-CoV-2-inactivated virus (B) after 6 d of stimulation; comparison of healthy controls (HC, *n* = 91 [A] or *n* = 46 [B]) with patients. For P6, cells were assessed at two independent time points 1 yr apart. Box plots are bound by the 25th and 75th percentiles with the median marked. The whiskers indicate the 5th and 95th percentiles, and outlier values are plotted. Unpaired *t* tests with Welch's correction were performed to compare the HC and patient groups. ****, *P* < 0.0001. (C–E) VirScan assay showing the presence of antibodies against viruses in the serum samples from patients and controls, with the analysis focusing on IAV (D) and coronaviruses (E). Data are representative of a single experiment. Adj Sp_score, adjusted species score; spp_RF, significant species response frequency; AbbPep, abbreviation of peptide (SpeciesName_ProteinName_UniprotID_start_end).

Table S1 is provided online and details the nine biallelic patient-associated IRF7 variants, all nonsynonymous or splicing site variants of IRF7 present in a homozygous state in at least one individual reported in the public gnomAD database, and all IRF7 variants present in a heterozygous state in the gnomAD database with an MAF >0.0001.

List of COVID Human Genetic Effort authors

Laurent Abel¹, Alessandro Aiuti², Saleh Al-Muhsen³, Fahd Al-Mulla⁴, Mark S. Anderson⁵, Evangelos Andreacos⁶, Andrés A. Arias⁷, Hagit Baris Feldman⁸, Alexandre Belot⁹, Catherine M. Biggs¹⁰, Dusan Bogunovic¹¹, Alexandre Bolze¹², Anastasiia Bondarenko¹³, Ahmed A. Bousfiha¹⁴, Petter Brodin¹⁵, Yenan Bryceson¹⁶, Carlos D. Bustamante¹⁷, Manish J. Butte¹⁸, Giorgio Casari¹⁹, John Christodoulou²⁰, Antonio Condino-Neto²¹, Stefan N. Constantinescu²², Megan A. Cooper²³, Clifton L. Dalgard²⁴, Murkesh Desai²⁵, Beth A. Drolet²⁶, Jamila El Baghdadi²⁷, Sara Espinosa-Padilla²⁸, Jacques Fellay²⁹, Carlos Flores³⁰, José Luis Franco³¹, Antoine Froidure³², Peter K. Gregersen³³, Bodo Grimbacher³⁴, Filomeen Haerynck³⁵, David Hagin³⁶, Rabih Halwani³⁷, Lennart Hammarström³⁸, James R. Heath³⁹, Sarah E. Henrickson⁴⁰, Elena W.Y. Hsieh⁴¹, Eystein Husebye⁴², Kohsuke Imai⁴³, Yuval Itan⁴⁴, Erich D. Jarvis⁴⁵, Timokratis Karamitros⁴⁶, Kai Kisand⁴⁷, Cheng-Lung Ku⁴⁸, Yu-Lung Lau⁴⁹, Yun Ling⁵⁰, Carrie L. Lucas⁵¹, Tom Maniatis⁵², Davood Mansouri⁵³, László Maródi⁵⁴, Isabelle Meyts⁵⁵, Joshua D. Milner⁵⁶, Kristina Mironska⁵⁷, Trine H. Mogensen⁵⁸, Tomohiro Morio⁵⁹, Lisa F.P. Ng⁶⁰, Luigi D. Notarangelo⁶¹, Antonio Novelli⁶², Giuseppe Novelli⁶³, Cliona O'Farrelly⁶⁴, Satoshi Okada⁶⁵, Keisuke Okamoto⁶⁶, Tayfun Ozcelik⁶⁷, Qiang Pan-Hammarström³⁸, Maria Papadaki⁶⁸, Jean W. Pape⁶⁹, Rebeca Perez de Diego⁷⁰, David S. Perlin⁷¹, Graziano Pesole⁷², Anna M. Planas⁷³, Carolina Prando⁷⁴, Aurora Pujol⁷⁵, Lluís Quintana-Murci⁷⁶, Sathishkumar Ramaswamy⁷⁷, Laurent Renia⁶⁰, Igor Resnick⁷⁸, Carlos Rodríguez-Gallego⁷⁹, Vanessa Sancho-Shimizu⁸⁰, Anna Sediva⁸¹, Mikko R.J. Seppänen⁸², Mohammed Shahrooei⁸³, Anna Shcherbina⁸⁴, Ondrej Slaby⁸⁵, Andrew L. Snow⁸⁶, Pere Soler-Palacín⁸⁷, András N. Spaan⁸⁸, Ivan Tancevski⁸⁹, Stuart G. Tangye⁹⁰, Ahmad Abou Tayoun⁷⁷, Stuart E. Turvey⁹¹, K M Furkan Uddin⁹², Mohammed J. Uddin⁹³, Diederik van de Beek⁹⁴, Donald C. Vinh⁹⁵, Horst von Bernuth⁹⁶, Joost Wauters⁹⁷, Mayana Zatz⁹⁸, Pawel Zawadzki⁹⁹, Helen C. Su⁶¹, Jean-Laurent Casanova¹⁰⁰

1. Laboratory of Human Genetics of Infectious Diseases, Necker Branch, INSERM U1163, Necker Hospital for Sick Children, Paris, France; University of Paris, Imagine Institute, Paris, France
2. San Raffaele Telethon Institute for Gene Therapy, IRCCS Ospedale San Raffaele, and Vita Salute San Raffaele University, Milan, Italy
3. Immunology Research Lab, Department of Pediatrics, College of Medicine, King Saud University, Riyadh, Saudi Arabia
4. Dasman Diabetes Institute, Department of Genetics and Bioinformatics, Dasman, Kuwait
5. Diabetes Center, University of California San Francisco, San Francisco, CA
6. Laboratory of Immunobiology, Center for Clinical, Experimental Surgery and Translational Research, Biomedical Research Foundation of the Academy of Athens, Athens, Greece
7. St. Giles Laboratory of Human Genetics of Infectious Diseases, Rockefeller Branch, The Rockefeller University, New York, NY; Primary Immunodeficiencies Group, Department of Microbiology and Parasitology, School of Medicine, University of Antioquia, Medellín, Colombia; School of Microbiology, University of Antioquia UdeA, Medellín, Colombia

8. The Genetics Institute, Tel Aviv Sourasky Medical Center and Sackler Faculty of Medicine, Tel Aviv University, Tel Aviv, Israel
9. Pediatric Nephrology, Rheumatology, Dermatology, HFME, Hospices Civils de Lyon, National Referee Center RAISE, and INSERM U1111, Université de Lyon, Lyon, France.
10. Department of Pediatrics, BC Children's and St. Paul's Hospitals, University of British Columbia, Vancouver, British Columbia, Canada
11. Icahn School of Medicine at Mount Sinai, New York, NY
12. Helix, San Mateo, CA
13. Shupyk National Medical Academy for Postgraduate Education, Kiev, Ukraine
14. Clinical Immunology Unit, Department of Pediatric Infectious Disease, CHU Ibn Rushd and LICIA, Laboratoire d'Immunologie Clinique, Inflammation et Allergie, Faculty of Medicine and Pharmacy, Hassan II University, Casablanca, Morocco
15. SciLifeLab, Department Of Women's and Children's Health, Karolinska Institutet, Stockholm, Sweden
16. Department of Medicine, Center for Hematology and Regenerative Medicine, Karolinska Institutet, Stockholm, Sweden
17. Stanford University, Stanford, CA
18. Division of Immunology, Allergy, and Rheumatology, Department of Pediatrics and the Department of Microbiology, Immunology, and Molecular Genetics, University of California, Los Angeles, CA
19. Clinical Genomics, IRCCS San Raffaele Scientific Institute and Vita-Salute San Raffaele University, Milan, Italy
20. Murdoch Children's Research Institute and Department of Paediatrics, University of Melbourne, Melbourne, Victoria, Australia
21. Department of Immunology, Institute of Biomedical Sciences, University of São Paulo, São Paulo, Brazil
22. de Duve Institute and Ludwig Cancer Research, Brussels, Belgium
23. Washington University School of Medicine, St. Louis, MO
24. Department of Anatomy, Physiology & Genetics, Uniformed Services University of the Health Sciences, Bethesda, MD
25. Bai Jerbai Wadia Hospital for Children, Mumbai, India
26. School of Medicine and Public Health, University of Wisconsin, Madison, WI
27. Genetics Unit, Military Hospital Mohamed V, Rabat, Morocco
28. Instituto Nacional de Pediatría (National Institute of Pediatrics), Mexico City, Mexico
29. School of Life Sciences, Ecole Polytechnique Fédérale de Lausanne, Lausanne, Switzerland; Precision Medicine Unit, Lausanne University Hospital and University of Lausanne, Lausanne, Switzerland
30. Research Unit, Hospital Universitario Nuestra Señora de Candelaria, Santa Cruz de Tenerife; CIBER de Enfermedades Respiratorias, Instituto de Salud Carlos III, Madrid; Genomics Division, Instituto Tecnológico y de Energías Renovables (ITER), Santa Cruz de Tenerife, Spain
31. Group of Primary Immunodeficiencies, University of Antioquia UDEA, Medellín, Colombia
32. Pulmonology Department, Cliniques Universitaires Saint-Luc ; Institut de Recherche Expérimentale et Clinique (IREC), Université Catholique de Louvain, Brussels, Belgium.
33. Feinstein Institute for Medical Research, Northwell Health USA, Manhasset, NY

34. Center for Chronic Immunodeficiency & Institute for Immunodeficiency, Medical Center, Faculty of Medicine, University of Freiburg, Freiburg, Germany
35. Department of Pediatric Immunology and Pulmonology, Centre for Primary Immunodeficiency Ghent (CPIG), PID Research Laboratory, Jeffrey Modell Diagnosis and Research Centre, Ghent University Hospital, Ghent, Belgium
36. The Genetics Institute Tel Aviv Sourasky Medical Center, Tel Aviv, Israel
37. Sharjah Institute of Medical Research, College of Medicine, University of Sharjah, Sharjah, United Arab Emirates
38. Department of Biosciences and Nutrition, Karolinska Institutet, Stockholm, Sweden.
39. Institute for Systems Biology, Seattle, WA
40. Department of Pediatrics, Division of Allergy Immunology, Children's Hospital of Philadelphia, Philadelphia, PA, USA; Department of Microbiology, Perelman School of Medicine, University of Pennsylvania, Philadelphia, PA
41. Departments of Pediatrics, Immunology and Microbiology, University of Colorado, School of Medicine, Aurora, CO
42. Department of Medicine, Haukeland University Hospital, Bergen, Norway
43. Department of Community Pediatrics, Perinatal and Maternal Medicine, Tokyo Medical and Dental University (TMDU), Tokyo, Japan
44. Institute for Personalized Medicine, Icahn School of Medicine at Mount Sinai, New York, NY, USA; Department of Genetics and Genomic Sciences, Icahn School of Medicine at Mount Sinai, New York, NY
45. Laboratory of Neurogenetics of Language and Howard Hughes Medical Institute, The Rockefeller University, New York, NY
46. Bioinformatics and Applied Genomics Unit, Hellenic Pasteur Institute, Athens, Greece
47. Molecular Pathology, Department of Biomedicine, Institute of Biomedicine and Translational Medicine, University of Tartu, Tartu Estonia
48. Chang Gung University, Taoyuan County, Taiwan
49. Department of Pediatrics & Adolescent Medicine, The University of Hong Kong, Hong Kong, China
50. Shanghai Public Health Clinical Center, Fudan University, Shanghai, China
51. Department of Immunobiology, Yale University School of Medicine, New Haven, CT
52. Zukerman Mind Brain Behavior Institute, Columbia University, New York, NY; New York Genome Center, New York, NY
53. Department of Clinical Immunology and Infectious Diseases, National Research Institute of Tuberculosis and Lung Diseases, The Clinical Tuberculosis and Epidemiology Research Center, National Research Institute of Tuberculosis and Lung Diseases (NRITLD), Masih Daneshvari Hospital, Shahid Beheshti, University of Medical Sciences, Tehran, Iran
54. Primary Immunodeficiency Clinical Unit and Laboratory, Department of Dermatology, Venereology and Dermatocology, Semmelweis University, Budapest, Hungary
55. Department of Pediatrics, University Hospitals Leuven; KU Leuven, Department of Microbiology, Immunology and Transplantation; Laboratory for Inborn Errors of Immunity, KU Leuven, Leuven, Belgium
56. Department of Pediatrics, Columbia University Irving Medical Center, New York, NY
57. University Clinic for Children's Diseases, Department of Pediatric Immunology, Medical Faculty, University "St. Cyril and Methodij" Skopje, North Macedonia

58. Department of Biomedicine, Aarhus University, Aarhus, Denmark
59. Tokyo Medical & Dental University Hospital, Tokyo, Japan
60. A*STAR Infectious Disease Labs, Agency for Science, Technology and Research, Singapore; Lee Kong Chian School of Medicine, Nanyang Technology University, Singapore
61. National Institute of Allergy and Infectious Diseases, National Institutes of Health, Bethesda, MD
62. Laboratory of Medical Genetics, IRCCS Bambino Gesù Children's Hospital, Rome, Italy
63. Department of Biomedicine and Prevention, Tor Vergata University of Rome, Rome, Italy
64. Comparative Immunology Group, School of Biochemistry and Immunology, Trinity Biomedical Sciences Institute, Trinity College Dublin, Ireland
65. Department of Pediatrics, Graduate School of Biomedical and Health Sciences, Hiroshima University, Hiroshima, Japan
66. Tokyo Medical and Dental University, Tokyo, Japan
67. Department of Molecular Biology and Genetics, Bilkent University, Bilkent - Ankara, Turkey
68. Center for Clinical, Experimental Surgery and Translational Research, Biomedical Research Foundation of the Academy of Athens, Athens, Greece
69. Haitian Study Group for Kaposi's Sarcoma and Opportunistic Infections (GHESKIO), Port-au-Prince, Haiti
70. Institute of Biomedical Research of IdiPAZ, University Hospital "La Paz", Madrid, Spain
71. Center for Discovery and Innovation, Hackensack Meridian Health, Nutley, NJ
72. Department of Biosciences, Biotechnology and Biopharmaceutics, University of Bari A. Moro, Bari, Italy
73. IIBB-CSIC, IDIBAPS, Barcelona, Spain
74. Faculdades Pequeno Príncipe, Instituto de Pesquisa Pelé Pequeno Príncipe, Curitiba, Brazil
75. Neurometabolic Diseases Laboratory, Bellvitge Biomedical Research Institute (IDIBELL), L'Hospitalet de Llobregat, Barcelona, Spain; Catalan Institution of Research and Advanced Studies (ICREA), Barcelona, Spain; Center for Biomedical Research on Rare Diseases (CIBERER), ISCIII, Barcelona, Spain
76. Human Evolutionary Genetics Unit, CNRS U2000, Institut Pasteur, Paris, France; Human Genomics and Evolution, Collège de France, Paris, France
77. Al Jalila Children's Hospital, Dubai, United Arab Emirates
78. University Hospital St. Marina, Varna, Bulgaria
79. Department of Immunology, University Hospital of Gran Canaria Dr. Negrín, Canarian Health System, Las Palmas de Gran Canaria; Department of Clinical Sciences, University Fernando Pessoa Canarias, Las Palmas de Gran Canaria, Spain
80. Department of Paediatric Infectious Diseases and Virology, Imperial College London, London, UK; Centre for Paediatrics and Child Health, Faculty of Medicine, Imperial College London, London, UK
81. Department of Immunology, Second Faculty of Medicine Charles University, V Uvalu, University Hospital in Motol, Prague, Czech Republic

82. Adult Immunodeficiency Unit, Infectious Diseases, Inflammation Center, University of Helsinki and Helsinki University Hospital, Helsinki, Finland; Rare Diseases Center and Pediatric Research Center, Children's Hospital, University of Helsinki and Helsinki University Hospital, Helsinki, Finland
83. Specialized Immunology Laboratory of Dr. Shahrooei, Ahvaz, Iran; Department of Microbiology and Immunology, Clinical and Diagnostic Immunology, KU Leuven, Leuven, Belgium
84. Department of Immunology, Dmitry Rogachev National Medical Research Center of Pediatric Hematology, Oncology and Immunology, Moscow, Russia
85. Central European Institute of Technology & Department of Biology, Faculty of Medicine, Masaryk University, Brno, Czech Republic
86. Department of Pharmacology & Molecular Therapeutics, Uniformed Services University of the Health Sciences, Bethesda, MD
87. Pediatric Infectious Diseases and Immunodeficiencies Unit, Vall d'Hebron Barcelona Hospital Campus, Barcelona, Catalonia, Spain
88. St. Giles Laboratory of Human Genetics of Infectious Diseases, Rockefeller Branch, The Rockefeller University, New York, NY; Department of Medical Microbiology, University Medical Center Utrecht, Utrecht, Netherlands
89. Department of Internal Medicine II, Medical University of Innsbruck, Innsbruck, Austria
90. Garvan Institute of Medical Research, Darlinghurst, New South Wales, Australia; St Vincent's Clinical School, Faculty of Medicine, UNSW Sydney, New South Wales, Australia
91. BC Children's Hospital, The University of British Columbia, Vancouver, Canada.
92. Centre for Precision Therapeutics, Genetics & Genomic Medicine Centre, NeuroGen Children's Healthcare and Lecturer, Holy Family Red Crescent Medical College Dhaka, Bangladesh
93. College of Medicine, Mohammed Bin Rashid University of Medicine and Health Sciences, Dubai, United Arab Emirates; Cellular Intelligence (Ci) Lab, GenomeArc Inc., Toronto, ON, Canada
94. Department of Neurology, Amsterdam Neuroscience, Amsterdam University Medical Center, University of Amsterdam, Amsterdam, Netherlands
95. Department of Medicine, Division of Infectious Diseases, McGill University Health Centre, Montréal, Québec, Canada; Infectious Disease Susceptibility Program, Research Institute, McGill University Health Centre, Montréal, Québec, Canada
96. Department of Pediatric Pulmonology, Immunology and Intensive Care, Charité Universitätsmedizin, Berlin University Hospital Center, Berlin, Germany; Labor Berlin GmbH, Department of Immunology, Berlin, Germany; Berlin Institutes of Health (BIH), Berlin-Brandenburg Center for Regenerative Therapies, Berlin, Germany
97. Department of General Internal Medicine, Medical Intensive Care Unit, University Hospitals Leuven, Leuven, Belgium
98. Biosciences Institute, University of São Paulo, São Paulo, Brazil
99. Molecular Biophysics Division, Faculty of Physics, A. Mickiewicz University, Poznań, Poland
100. The Rockefeller University & Howard Hughes Medical Institute, New York, NY; Necker Hospital for Sick Children & INSERM, Paris, France